Sedimentologika

Research article

Distinguishing climate and tectonic signals in the stratigraphy of the Kura Basin, the southeastern foreland of the Greater Caucasus

Kristoffer Fowler* & Adam M. Forte*

Department of Geology and Geophysics, Louisiana State University, Baton Rouge, LA, USA

*corresponding authors: Kristoffer Fowler (kfowl11@lsu.edu)

doi: 10.57035/journals/sdk.2024.e21.1272

Editors: Peter Burgess and Julien Bailleul
Reviewers: Larry Syu-Heng Lai and Sergei Lazarev
Copyediting, layout and production: Romain Vaucher, Liz Mahon and Faizan Sabir

Submitted: 24.09.2023
Accepted: 14.04.2024
Published: 10.07.2024

Abstract | Assessing the relative contributions of tectonics and climate in orogenic systems and the stratigraphy preserved within their fringing basins has guided research for decades. Determining the role of these contributions is non-trivial and is difficult due to variations in both magnitude and period over which fluctuations in tectonics and climate occur, typically $\geq 10^{5-7}$ years and $<10^{5}$ years, respectively. The Greater Caucasus is a young orogen that offers a unique opportunity to assess these critical roles through analysis of exposures of the foreland stratigraphy. Here, we synthesize available measured stratigraphic sections from within the Kura Fold-Thrust Belt and adjoining regions, creating multiple paleogeographic reconstructions for key regional chronostratigraphic stages, and then assessing the Kura Basin's response time throughout these stages. We use basin response time as a proxy for whether tectonics or climate fluctuations could be preserved within the Kura Fold-Thrust Belt stratigraphy and, thus, what changes in depositional environments during those periods are more likely to reflect. In general, estimates of basin response times indicate that tectonic signals could be preserved throughout the Kura Basin during the deposition of the Productive Series. Climatic signals would likely be preserved during the deposition of the Akchagyl stage, although tectonics signals cannot be ruled out. During the Apsheronian stage, both tectonic and climate signals can be preserved. These results highlight that a foreland basin system can fluctuate between being able to record mixtures of tectonic and climatic signals during both different geologic stages and within the same stage across a foreland.

Lay summary | The sedimentary rock record records the interactions between tectonic and climatic forces during mountain formation, which is key for interpreting the rock record, but tectonics and climate tend to operate on fundamentally different timescales, making interpreting this a difficult task. By analyzing the sedimentary rock record in the basins adjacent to mountains, we can evaluate which of these forces are more likely to be preserved. The actively developing Greater Caucasus offers a unique study area to explore the preservation potential of climatic vs. tectonic signals because of the relatively well-exposed sedimentary rock record adjacent to the range. Our synthesis of published records of sedimentary rocks within the southeastern basin of the Greater Caucasus suggests that the basin shifts over time from being able to record tectonic forces to climatic forces to possibly recording both simultaneously. The results from the Greater Caucasus are useful for considering the variability of the type of environmental signals that might be preserved in other basins adjacent to mountain ranges. Our new synthesis also has the added benefit of compiling decades' worth of work done within the southeastern Greater Caucasus foreland basin in a single place, allowing us to create a series of maps from the past that show how the environments adjacent to the mountain range changed throughout time.

Keywords: Greater Caucasus, Kura Basin, Environmental Signals, Foreland Basin, Stratigraphy

1. Introduction

Distinguishing between tectonic or climatic signals within foreland basin stratigraphy can be challenging because both forcings can generate similar environmental signals, e.g., changes in sediment flux, provenance switches, grain size fluctuations, subsidence rates, etc. (Armitage et al., 2011; Allen et al., 2013; Romans et al., 2016; Caracciolo,

This is an open access article under the terms of the Creative Commons Attribution License (CC-BY) © 2024 The Authors

2020; Caracciolo et al., 2021; Ravidà et al., 2021; Tofelde et al., 2021). These environmental signals generated in the upstream i.e., erosional portion, of a sedimentary system propagate downstream through the transfer zone and then eventually to the permanent sink, i.e., the basin, during which the signal can be faithfully transmitted or muted by sedimentary processes occurring throughout the sediment routing system (Castelltort & Van Den Driessche, 2003; Romans et al., 2016). Disentangling which environmental signals are preserved within a sedimentary basin and what they represent is a non-trivial task that is complicated by numerous factors, including (1) differences in the timescales of tectonic (e.g., orogenesis) (10^5 – 10^7 years) and climatic (e.g., Milankovitch Cyclicity) ($<10^5$ years) perturbations that often occur in tandem and are superimposed on each other; (2) sediment storage within the transfer zone leading to variable lag times; and (3) geomorphic processes in the transporting rivers and the overall fluvial regime within the basin can variably "shred" these environmental signals (Allen et al., 2013; Romans et al., 2016; Tofelde et al., 2021). In general, there are two broad types of response times: the basin response time and the response time of the erosion zone to a change in the sediment flux in a fluvial system. A first-order technique to assess the likelihood of a potential signal type being preserved or lost in the sedimentary record is the basin's response time. In a simple sense, the basin response time is how reactive or buffered a sedimentary system's response is to a change in one of its boundary conditions, and is the amount of time it would take a 1D profile of a fluvial system to reach equilibrium after a change in the surrounding tectonic and/or climatic regime (Heller & Paola, 1992; Paola et al., 1992; Romans et al., 2016; Tofelde et al., 2021). In contrast, if the perturbation timescale is less than the basin response time, an environmental signal propagating through the system will likely be buffered, decreasing the "amplitude" of the signal or potentially completely shredding the signal so that it is not recorded (Romans et al., 2016). A similar scenario occurs when considering the response of the erosion zone to fluctuations in the boundary conditions in that the sediment flux for a given time is dependent on the frequency of the perturbation within the sediment source (e.g., Stevens Goddard et al., 2020). While the basin response time is controlled by a variety of factors, it is the most sensitive to the length scale of the basin (Paola et al., 1992; Castelltort & Van Den Driessche, 2003; Romans et al., 2016), and thus, accurate reconstructions of basin geometry and depositional environments through time is critical for assessing response times within foreland basins.

Here we apply these concepts to the Kura Basin (KB) along the southeastern edge of the actively deforming Greater Caucasus (GC) mountains to evaluate the extent to which we expect climate and tectonic signals to be preserved within this foreland. The GC is an ~1000 km long approximately NW-SE trending orogen that is the product of the ongoing NNE collision of the Arabian (Ab) and Eurasian (Eu) plates (Adamia et al., 1977; Allen et al., 2004; Adamia et al., 2011a, 2011b). Low-temperature thermochronology indicates that the GC orogen is relatively young, with rapid exhumation beginning between 10 – 5 Ma, with long-term average exhumation rates exceeding 1 mm/yr within the core of the orogen (Avdeev & Niemi, 2011; Vincent et al., 2020; Forte et al., 2022a; Tye et al., 2022), and millennial-scale exhumation rates up to ~8 mm/yr (Forte et al., 2022b). Over this same period of time, the Caucasus region has experienced a variety of significant climatic perturbations (e.g., Milanovsky, 2008; Lazarev et al., 2021; Vasiliev et al., 2022) and large-scale base-level variations of the adjoining Caspian, and to a lesser extent, Black Seas (e.g., Reynolds et al., 1998; Green et al., 2009; Krijgsman et al., 2019; Van Baak et al., 2019; Lazarev et al., 2021). Late Cenozoic stratigraphy of the Kura foreland basin, whose depositional period spans the timing of many of these first-order climatic and tectonic perturbations, is exposed within the actively deforming Kura Fold -Thrust Belt (KFTB) (Forte et al., 2010, 2013b, 2015a; Alania et al., 2018; Sukhishvili et al., 2021) and further east in other GC related structures (Vincent et al., 2010; Van Baak et al., 2013, 2019; Richards et al., 2018; Jorissen et al., 2020), providing a potentially rich record of both tectonically and climatically generated signals. Much of the exposed stratigraphy exhibit significant variability in depositional environments on a variety of temporal and spatial scales, which have been interpreted in terms of either tectonic (Forte et al., 2013b, 2015a) or climatic forcing (Van Baak et al., 2013; Hoyle et al., 2020; Jorissen et al., 2020; Lazarev et al., 2019, 2021). However, the lack of detailed paleoclimate work within the KB and uncertainties with respect to the timing of major tectonic events within the GC (Forte et al., 2022a; Trexler et al., 2022; Tye et al., 2022) or KFTB (Sukhishvili et al., 2021) makes assessing the veracity of interpretations of climatic or tectonic forcing from the stratigraphy problematic.

To address this, here we capitalize on the significant recent work (e.g., Jorissen et al., 2020; Lazarev et al., 2019, 2021) defining, dating, and describing stratigraphy within the KFTB and adjoining regions to synthesize available published measured sections into a coherent framework. We focus on correlating the KB stratigraphy along strike within the GC foreland and synthesizing depositional environmental interpretations to produce paleogeographic reconstructions that take into account motion of associated tectonic blocks based on recent plate reconstructions (van der Boon et al., 2018; van Hinsbergen et al., 2020). This is complimentary to recent efforts by Aghayeva et al. (2023) to reconstruct paleogeography of the GC region for much of the pre-tectonic period. In our case, we use our paleogeographic reconstructions along with conservative estimates of paleoclimate to estimate the spatial and temporal variation in basin response time throughout the KB. Our results have implications for the expected likelihood of a given signal, i.e., climatic vs tectonic, to be preserved in different parts of the basin during the uplift of the GC and major base-level fluctuations of the Caspian Sea.

2. Geologic Setting

The stratigraphy and basin history that we synthesize here is fundamentally a reflection of both the regional tectonic and climatic history, and as such, we first provide an overview of the major tectonic and climatic fluctuations that have occurred, or still are occurring, in and around the Caucasus. For the tectonics portion of the synthesis, information on both the collision between Ab-Eu and local tectonics of the KB and KFTB is provided. The climatic fluctuations are also presented in a similar macro (regional) and micro (local) order. The primary difference being that some regional scale climatic shifts are possibly linked to far-field changes in the global climate or beyond the Caucasus region itself.

2.1. Arabia – Eurasia Collisional Tectonics

The Ab – Eu indenter tectonics resulted in key paleo-geographic and tectonic development both within the Caucasus and adjacent areas spanning from Iran to Turkey, and in a broad scope is a key component of the Alpine-Himalayan orogenic belt (Axen et al., 2001; Allen & Armstrong, 2008; Cowgill et al., 2016; Barber et al., 2018; Darin & Umhoefer, 2022). The formal boundary of the Ab – Eu collision is marked by the Bitlis – Zagros suture, which is a result of the closure of the Neotethys Ocean. As a result of this closure, several major orogenic belts have developed over the last 40 Ma, with significant deformation occurring >500 km north of the suture zone. Relative to the Bitlis – Zagros suture, these include the Zagros mountains to the ESE, Zagros Fold-Thrust Belt to the south, the Alborz to the ENE, the GC and the KFTB to the north, and the westward tectonic extrusion of Anatolia (Axen et al., 2001; Ballato et al., 2011; Darin & Umhoefer, 2022). These collisions, coupled with the collision between the Indian sub-continent and Eurasia and Africa in east and west respectively, resulted in the segmentation of the Western Tethys Ocean and subsequent formation of the Eocene to Miocene Paratethys Sea (Rögl, 1999). The Paratethys Sea was an epicontinental sea that stretched from modern-day western Europe into Asia (Rögl, 1999). In particular, the Ab – Eu collision primarily affects the eastern portion of the Paratethys Sea resulting in the formation of several basins found around the circum-Caucasus regions in the Eastern Paratethys Sea (e.g., the Black Sea and South Caspian Basins) (Rögl, 1999; Popov et al., 2006). In this Ab – Eu collisional system, the GC is the northernmost and one of the youngest topographic expressions, and as such plays an important role in accommodating the on-going Ab – Eu collision (Zonenshain & Pichon, 1986; Philip et al., 1989; Allen et al., 2004). Additionally, the GC and KFTB are key to understanding the on-going convergence between Ab – Eu, with most of the convergence from ~10 Ma – 5 Ma accommodated by thrusts along the southern range front of the GC (Trexler et al., 2022, 2023).

2.2. Local Tectonics of the Kura Basin and the Kura Fold-Thrust Belt

2.2.1. Local Tectonics of the Kura Basin

The KB is currently separated from the GC along its northern border by the KFTB and the piggyback Alazani Basin and bordered to the south by the Lesser Caucasus (LC) (Figures 1 and 2). Due to the KB's position atop the northward under-thrusting LC margin, it is considered the eastern pro-foreland basin of the GC and is a western subbasin of the South Caspian Basin (Koçyiğitet al., 2001; Ershov et al., 2003; Forte et al., 2010). Within the KB, the basin fill ranges from ~5 – 8 km in thickness, with most of the sediment since the Pliocene eroded from GC and LC sources (Morton et al., 2003; Forte et al., 2010, 2015a, 2023; Abdullayev et al., 2018; Tye et al., 2020; Tari et al., 2021).

Like other Paratethyan main basin-subbasin pairs, there is a significant difference in the thicknesses between the Cenozoic sedimentary fill of the KB, as the South Caspian Basin fill is 15 - 20 km thick (Jackson et al., 2002; Green et al., 2009; Gunnels et al., 2020; Tari et al., 2021). The KB – South Caspian Basin sediment thickness disparity reflects that: (1) the KB is the sub-basin fringing the super-deep South Caspian Basin, which has resulted in the South Caspian Basin being the primary sediment sink during Caspian Sea low stands (Kroonenberg et al., 2005; Green et al., 2009; Forte et al., 2015a; Abdullayev et al., 2018); (2) the KB was originally thought to be underlain by Jurassic – Cretaceous island-arc material (e.g., Green et al., 2009), but more recent studies by Gunnels et al. (2020) have found the underlying crust of the KB to be a continuation of the South Caspian Basin's crustal composition, interpreted as being either overly-thinned continental crust, or overly-thickened oceanic crust (Zonenshain & Pichon, 1986; Ershov et al., 2003; Egan et al., 2009; Green et al., 2009; McKenzie et al., 2019; Gunnels et al., 2020); (3) the South Caspian Basin has a relatively complex subsidence history driven by the interplay of post Jurassic – Cretaceous thermal subsidence, Eocene – Oligocene flexural subsidence induced by the Ab – Eu collision, flexural loading driven by the late Miocene – early Pliocene onset of north-directed subduction underneath the Apsheron Peninsula, and the rapid uplift of the GC initiating in the Mio-Pliocene (Allen et al., 2002; Jackson et al., 2002; Egan et al., 2009; Green et al., 2009; Avdeev & Niemi, 2011; Forte et al., 2022a); (4) the paleo-Kura, Amu Draya, and Volga rivers all emptied directly into the South Caspian Basin or along the fringes of the South Caspian Basin, resulting in the deposition of 5 – 8 km of sediment in ~2.5 Ma (Jones & Simmons, 1997; Reynolds et al., 1998; Hinds et al., 2004; Abdullayev et al., 2018); and (5) along the western extent of the South Caspian Basin, the West Caspian Fault with a mixture of dextral ENE thrusting is likely placing a flexural load on the South Caspian Basin lithosphere, and accommodating differential rates of subsidence between the KB and South Caspian Basin (Kadirov et al., 2012)

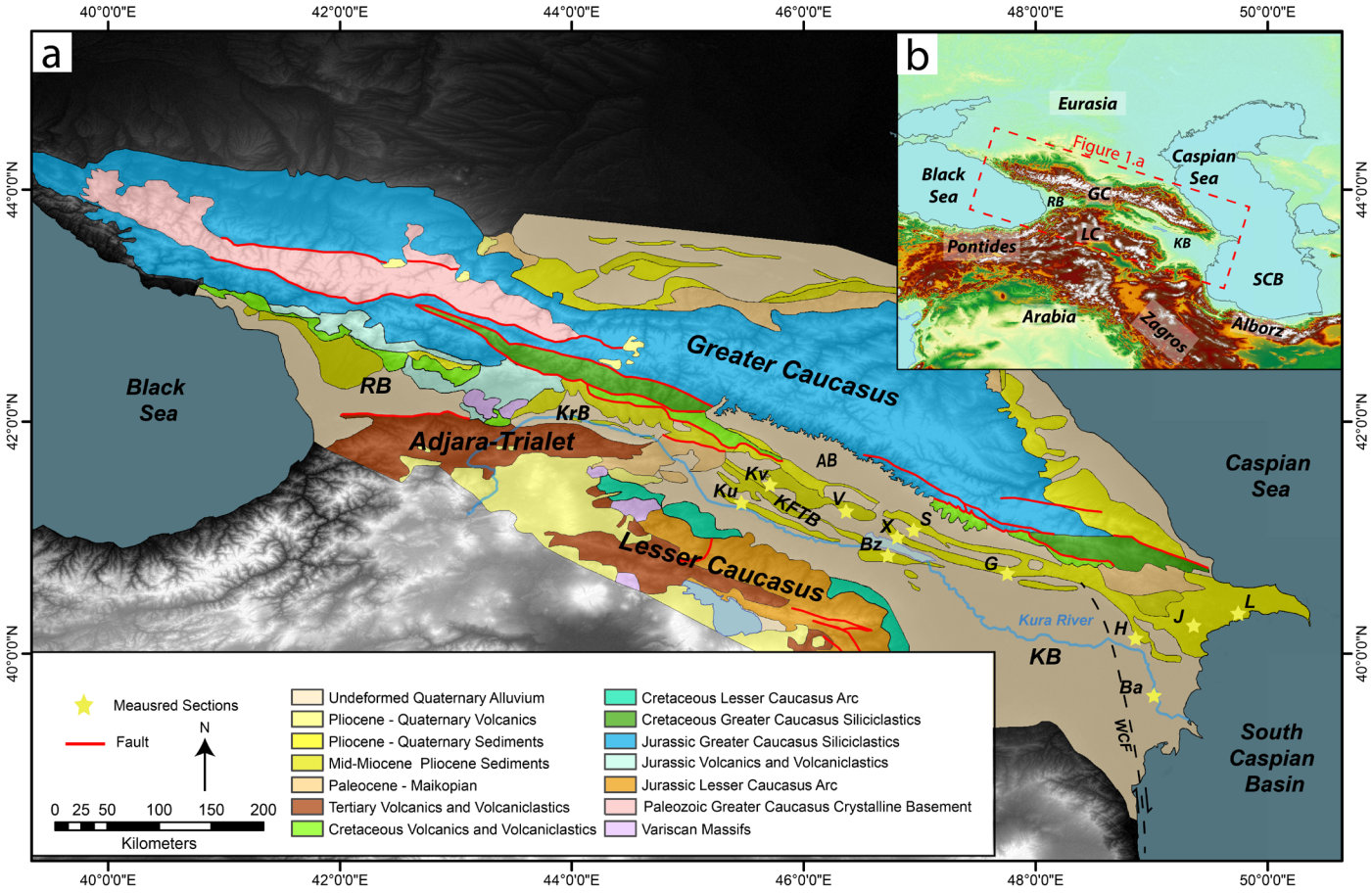

Figure 1 | Panel (A) Geologic map of the Caucasus. Panel (B) Geographic map of the circum-Caucasus region. Dashed red polygon indicates extent of panel (A). (A) GC = Greater Caucasus, LC = Lesser Caucasus, KB = Kura Basin, RB = Rioni Basin, KrB = Kartli Basin, AB =Alazani Basin, KFTB = Kura Fold-Thrust Belt, SCB = South Caspian Basin. Measured sections: L = Lokbatan, J= Jeirankechmez, H = Hajigabul, Ba = Babazanan, G = Gӧychay, S = Sarica, X = Xocashen, Bz = Bozdagh, V = Vashlovani, Kv = Kvabebi, Ku = Kushkuna, WCF = West-Caspian Fault.

The geometry of the KB is unlike typical pro-foreland basins where the deepest portion of the foredeep is located proximal to the topographic load (e.g., DeCelles & Giles, 1996). Instead, the KB is at its deepest at the front edge of the KFTB, with the basin depth decreasing approaching the LC (Ershov et al., 2003; Nemčok et al., 2013), though explanations for this geometry remain enigmatic. Exposed sediment within the KFTB reflect both pre- and syn-tectonic histories during the uplift of the GC and KFTB activation. As such, here we refer to all sediment exposed within the KFTB generically as being deposited in the KB even though some likely reflect deposition within intermontane basins of the KFTB, a point we return to in our stratigraphic synthesis. In general, most of the of the exposed strata within the KFTB are Plio-Pleistocene and include those defined locally as the Productive Series, Akchagyl, and Apsheron stages, with the latter two stages making up 27% and 43% of the exposed stratigraphy within the presented measured sections, respectively. In turn, these stages are key for both tectonic and paleoenvironmental interpretations made in previous work as they span several large Caspian Sea base-level fluctuations, the initiation of rapid uplift of the GC, and the development of the KFTB (Vincent et al., 2010; Forte et al., 2013b, 2015a; Van Baak et al., 2013, 2019; Jorissen, 2020; Jorissen et al., 2020; Lazarev et al., 2019, 2021; Sukhishvili et al., 2021).

2.2.2. Local Tectonics of the Kura Fold-Thrust Belt

Activation of the KFTB represents a southward propagation of the GC deformation front and at least partial deactivation of former southern rangefront deformation structures that previously accommodated the convergence between Ab – Eu (Mosar et al., 2010; Forte et al., 2010, 2013b, 2015a; Cowgill et al., 2016). In detail, it is estimated that since its activation, the KFTB has accommodated between 80 – 100% of the convergence between the GC and LC, and approximately half of the Ab – Eu collision at the longitude of the eastern GC (Forte et al., 2010, 2013b; Sukhishvili et al., 2021). However, the exact timing and the patterns of the KFTB initiation remain enigmatic. Forte et al. (2010) suggested that the thrust belt initiated diachronously, propagating eastward based on the Akchagyl – Apsheron boundary, appearing to be pre-tectonic in the west and syn-tectonic in the east. However, this hypothesis was posed before it was recognized that many of the stage boundaries within the KB may be time-transgressive (e.g., Forte et al., 2015a). Subsequent work refining the ages of the Akchagyl – Apsheron boundary in the eastern KFTB by Lazarev et al. (2019) implies that the KFTB initiated between 2.2 Ma – 2.0 Ma near its eastern terminus. Near its western terminus, Sukhishvili et al. (2021) bracketed the uplift of the Gombori range along the northwestern flank of the KFTB to 2.7 Ma – 1.0 Ma.

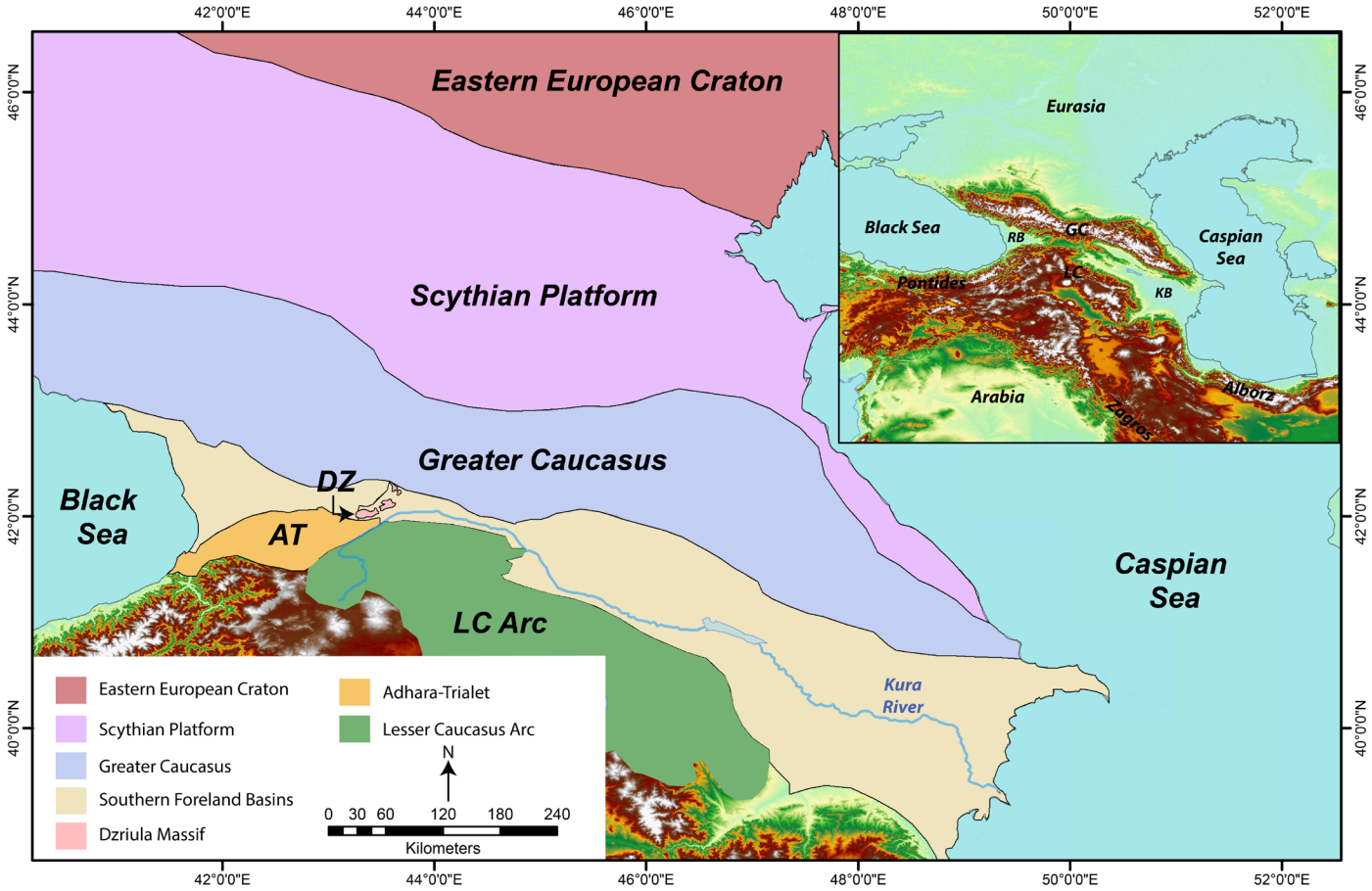

Figure 2 | Tectonic map of the Caucasus. DZ = Dzirula Massif, AT = Adhara - Trialet, LC = Lesser Caucasus.

Most recently, sediment provenance work by Forte et al. (2023) within the central KFTB suggests that an observed divergence of different provenance signals within the Plio-Pleistocene stratigraphy reflects the onset of significant intra-fold-thrust belt sediment recycling caused by the initiation of the KFTB at ~2 Ma. Together, these results imply a significant potential overlap in timing between the western, central, and eastern KFTB, and are permissive of effectively synchronous initiation along strike. Ultimately, better understanding of the stratigraphic framework of the northern KB as exposed in the KFTB is required to make additional progress in bracketing the structural history of the KFTB, and in turn, the Plio-Pleistocene tectonic history of the central and eastern GC.

The KFTB not only has importance in regional tectonics, but its geometry and history has also influenced localized exposures of Mio-Pliocene (pre-tectonic) stratigraphy, and the deposition of younger (syn-tectonic) Pleistocene-Quaternary stratigraphy. The control on the exposure is both dependent on the thickness of individual stratigraphic units across the basin, and depth of the detachment within the KB. The location of this detachment across the KB is generally considered to be within the Oligocene Maykopian gypsums and clays (Adamia et al., 2011b; Alania et al., 2017, 2018) but the exact depth of the detachment varies across the KB. In the central-western portion of the KB, the depth of the shallow-level detachment is ~8 km and soles into the Upper Sarmatian, exposing older strata (e.g., Sarmatian and Meotian – Pontian) in the regions of Vashlovani and the Didi Shiraki Piggyback Basin (Forte et al., 2015a; Alania et al., 2017, 2018). In the eastern extent of the KFTB, the shallow detachment soles to a depth of ~4 – 5 km into the Akchagyl – Apsheron stages, exposing mostly Pleistocene – Quaternary stratigraphy (e.g., Forte et al., 2010, 2013b).

2.3. Caspian Sea Base Level and Mechanisms

Throughout the Pliocene to Pleistocene, the stratigraphy of the KB was influenced by base-level fluctuations within the Caspian Sea, which itself was influenced by multiple factors including; ephemeral connections with the Black Sea and open marine environments, the water budget within the major Caspian Sea drainage basins, far-field changes in Atlantic Ocean thermohaline circulation, possibly large scale hyper-aridity of northern Arabia, and the late Plio-Pleistocene glaciation of the GC and circum-GC area (Milanovsky, 2008; Forte et al., 2013a; Van Baak et al., 2013, 2017, 2019; Richards et al., 2018; Jorissen, 2020; Jorissen et al., 2020; Lazarev et al., 2019, 2021; Hoyle et al., 2020, 2021). Importantly, the size of some of these Caspian Sea base-level changes are several orders of magnitude greater than eustatic sea-level change, and thus can have a large influence on the stratigraphy of surrounding regions. For example, the Pliocene Productive Series (5.35 Ma to 2.95 Ma) marks a drastic Caspian Sea regression of ~-600 m - -1500 m below the modern base-level of the Caspian Sea (Reynolds et al., 1998; Kroonenberg et al., 2005; Forte et al., 2013a; Van

Baak et al., 2013). This Caspian Sea regression resulted in both the restriction of the entire Caspian Sea within the South Caspian Basin, and the southern migration of the Volga delta several hundred kilometers south, to the position of the Apsheron Sill and Peninsula (Kroonenberg et al., 2005; Green et al., 2009). Several mechanisms have been proposed for the isolation of the Caspian Sea within the South Caspian Basin, including thermal subsidence of the underlying South Caspian basement, rapid sediment loading of the lithosphere, or loading of the lithosphere due to north-directed subduction beneath the Apsheron Sill (Allen et al., 2002; Jackson et al., 2002; Ershov et al., 2003; Egan et al., 2009; Green et al., 2009; Van Baak et al., 2013).

Similarly, multiple mechanisms have been proposed for the large magnitude Caspian Sea transgression and marine connection that followed the Productive Series, i.e., the Pleistocene Akchagylian stage within the Caucasus region. There are two proposed, plausible hydrologic mechanisms for this significant expansion of the Caspian Sea in the Pleistocene: (1) the influx of marine Arctic Ocean water into the Caspian Sea via the expansion of the Barents and Scandinavian ice sheets between ~2.7 Ma – 2.75 Ma, resulting in isostatic loading and the inundation of channels towards the Caspian Sea (Van Baak et al., 2019) or (2) a net positive water budget over the Caspian Sea drainage basins (Lazarev et al., 2021). Evidence for mechanism 1 derives from observations of the first appearance of Arctic marine foraminifera, with temporal constraints provided by Ar^{40}/Ar^{39} dating of multiple ash beds from the lowermost Akchagylian within the Jeirankechmez section on the Apsheron Peninsula (Figure 1; Richards et al., 2018; Krijgsman et al., 2019; Van Baak et al., 2019). Evidence for mechanism 2 comes from new magnetostratigraphic and radiometric dating results from the Kvabebi, Hajigabul, and Kushkuna sections (Figure 1) that document Akchagylian deposits occur earlier than 2.7 Ma and thus resulted in the increase in the age of the lower boundary of the Akchagylian stage (Lazarev et al., 2021). Lazarev et al. (2021) incorporate their new chronologic constraints with palynological work by Richards et al. (2018), Hoyle et al. (2021), and stratigraphic interpretations by Jorissen (2020) and Jorissen et al. (2020), which, when incorporated, results in freshwater – brackish water Akchagylian deposits near the Akchagylian transgressive surface and the placement of the lower Akchagylian boundary at 2.95 Ma (Lazarev et al., 2021). The presence of freshwater to brackish water conditions at the base of the Akchagylian stage provides support for mechanism 2, as a positive water budget would allow for freshwater conditions to inundate the KB. The origin of this positive water budget within the Caspian Sea region is possibly related to the warming of the Atlantic Thermohaline Circulation, driving moisture further into the Eastern European Craton, including into the Caspian Sea drainage basins (Bartoli et al., 2005; Lazarev et al., 2021).

2.4. Climatic Conditions

2.4.1. Greater Caucasus Climatic Setting

2.4.1.1. Greater Caucasus Precipitation Gradient

In the modern, the GC has a prominent, along-strike climatic gradient, thought to primarily reflect the eastward moisture transport by the Westerlies from the Black Sea and central Europe (Borisov et al., 1965; Lydolph, 1977; Forte et al., 2016, 2022b). This interaction with the Westerlies results in an eastward decrease in precipitation from ~4 – 6 mm/day near the Black Sea coast to ~1 mm/day near the Caspian Sea coast (Figure 3; Forte et al., 2016, 2022b). The precipitation gradient is most prominent at low elevations and in the foreland basins, with a less extreme gradient at higher elevations within the range (Forte et al., 2016). There are insufficient paleoclimatic records within foreland basins of the GC to determine whether this precipitation gradient pre-dates development of the range or grew in concert with the topography.

2.4.1.2. Greater Caucasus Glaciation

The Pliocene to present-day GC has a variable history of glaciation periods along the main range. In general, the duration of individual GC glaciation events decrease from the Pliocene into the late Pleistocene, with the longest glaciation event being the Elbrus glaciation that spanned ~700 kya, occurring during MIS stages KM6 – G8 (Figure 4; Milanovsky, 2008). The next longest event was the Chegem glaciation during the Pleistocene for ~300 kya across MIS stages 92 – 78 (Figure 4; Milanovsky, 2008). The remaining Pleistocene glaciation events occur over significantly shorter time spans from 250 kya to <40 kya (Figure 4; Milanovsky, 2008).

The extent of modern GC glaciers decreases from west to east due primarily to a decrease in the available precipitation as a result of the previously described precipitation gradient (Gobejishvili et al., 2011). During the late Pleistocene, glaciation in the western GC terminated between 600 – 1800 m above sea level, and in the eastern GC glaciation terminate at higher elevations between 1200 – 2400 m above sea-level (Gobejishvili et al., 2011). Importantly, the topography of the GC does not bear characteristic signatures of being strongly influenced by glacial erosion (e.g., Brocklehurst & Whipple, 2004). Thus, prior work has broadly considered that erosion and sediment generation with the GC is dominated by fluvial processes (Forte et al., 2014), though detailed work on sediment provenance considered glacial outburst floods and associated debris flows to be an important erosional and sediment generation mechanism in the range (Vezzoli et al., 2020).

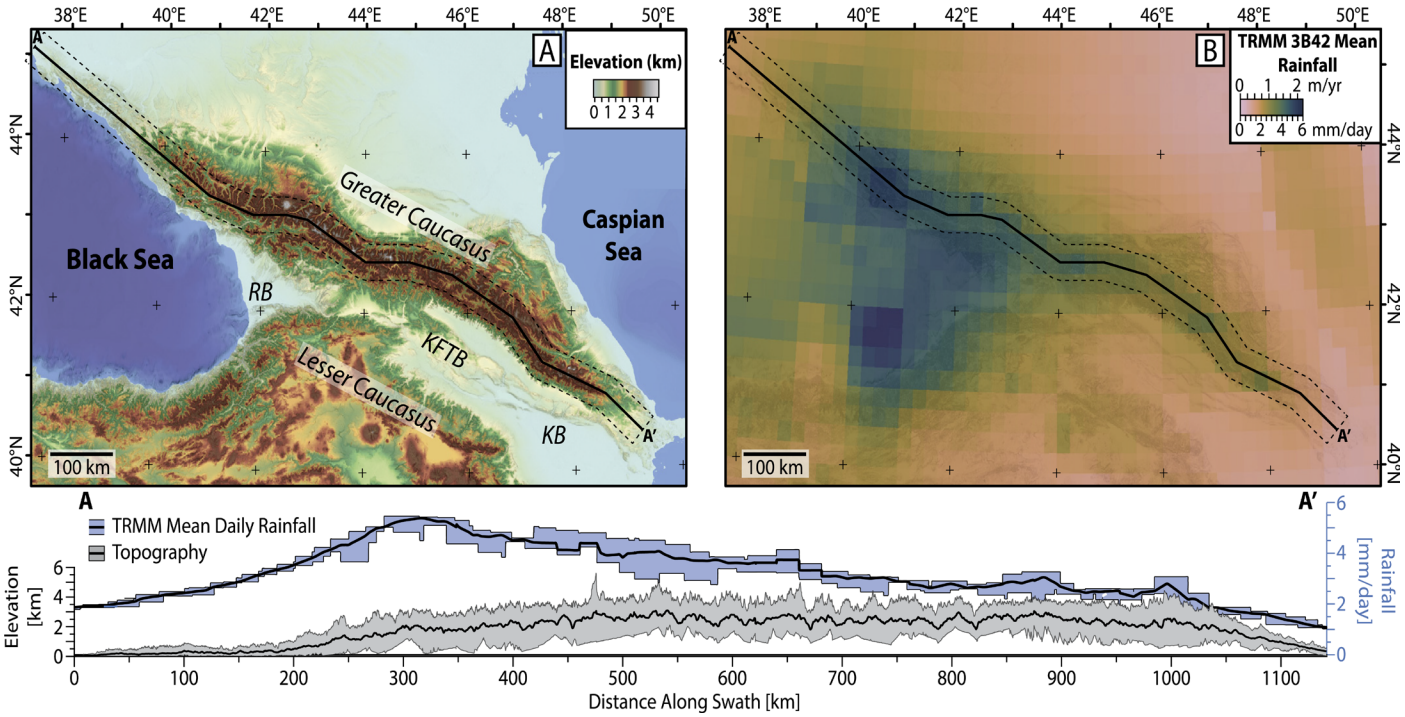

Figure 3 | Modified from Forte et al. (2022). Panel (A) is a DEM of the Caucasus DEM of the Caucasus displaying regional elevations with the same abbreviations in panels (A) & (B) from Figure 1. A – A′ is the same as in the profiles below panels (A) and (B), with the centerline of the profile being centered along the topographic crest of the Greater Caucasus with a 50 km width swath on either side marked by the dashed polygon. Panel (B) is measurements made by the Tropical Rainfall Measurement Mission (TRMM 3B42) from Forte et al. (2016). A – A′ is the same as in Panel (A). Swaths below: In grey are the results of the A – A′ elevation along the main range, and in blue are the along A – A′ variations in the mean daily rainfall.

2.4.2. Climatic Events in and Around the Circum-Caspian Region

Two significant regional climatic events occurred during the deposition of the late Pontian and Productive Series Caspian stages, specifically the Messinian Salinity Crisis (MSC) and the North Arabian Desert Climax (NADC) (Figure 4). The Messinian Salinity Crisis (5.96 Ma – 5.33 Ma) refers to the period in which tectonic closure of the gateway between the Atlantic Ocean and the Mediterranean Sea resulted in the extreme desiccation of the Mediterranean Sea (Hsü et al., 1977; Krijgsman et al., 1999). This event primarily occurred during the Pontian stage of the Caspian, and was once considered to be a plausible causal mechanism for the Caspian regression during the Productive Series stage (Jones & Simmons, 1997). However, due to the lack of connection between the Caspian Sea, the Black Sea and Mediterranean Sea at this time, the Paratethys likely had a positive water budget. While there is direct evidence that the paleo-Volga was still actively contributing to the South Caspian Basin into the Pliocene, subsequent work has indicated there is, at best, a weak connection between the MSC and Productive Series (de la Vara et al., 2016; Van Baak et al., 2017).

The next event was North Arabian Desert Climax (NADC) (5.59 Ma – 3.3 Ma), which marks a period of hyper-aridity within northeast Africa and Arabia (Figure 4; Böhme et al., 2021). However, despite the regional proximity, there is no direct evidence that this event influenced the Caucasus region. Due to the lack of apparent direct connection of either the MSC or NADC to the climate and/or stratigraphy of the Caucasus region, we do not consider them further in our interpretations.

2.5. Stratigraphic Framework of the Kura Basin

A relatively well established regional to local biostratigraphic framework tied to base level variations of the Caspian Sea exists for the circum-Caucasus region (Jones & Simmons, 1997); however, correlation of these regional states to the global timescale, and thus establishing absolute ages of the stage boundaries, have proven problematic (Van Baak et al., 2013; Krijgsman et al., 2019 and references therein). In particular, efforts to establish absolute age control within the central KB are hindered by 1) a lack of widely distributed and/or dateable ash beds, 2) extreme spatial variability in depositional environments such that lithostratigraphic correlation is not feasible, and 3) the endemic nature of microfossil assemblages (Forte, 2012; Forte et al., 2015a; Richards et al., 2018; Van Baak et al., 2019). However, placing the local biostratigraphy within a magnetostratigraphic context has proven a reliable method to correlate the KB and KFTB stratigraphy with the global timescale (Krijgsman et al., 2019). Ultimately, the absolute age and definition of the upper and lower boundaries of the Caspian stages are critical for bracketing the timing of important tectonic and basin-wide events e.g., the timing of the Akchagylian flood, and activation of the KFTB (Forte et al., 2013b, 2015a; Van Baak et al., 2019; Lazarev et al., 2019, 2021; Sukhishvili et al., 2021).

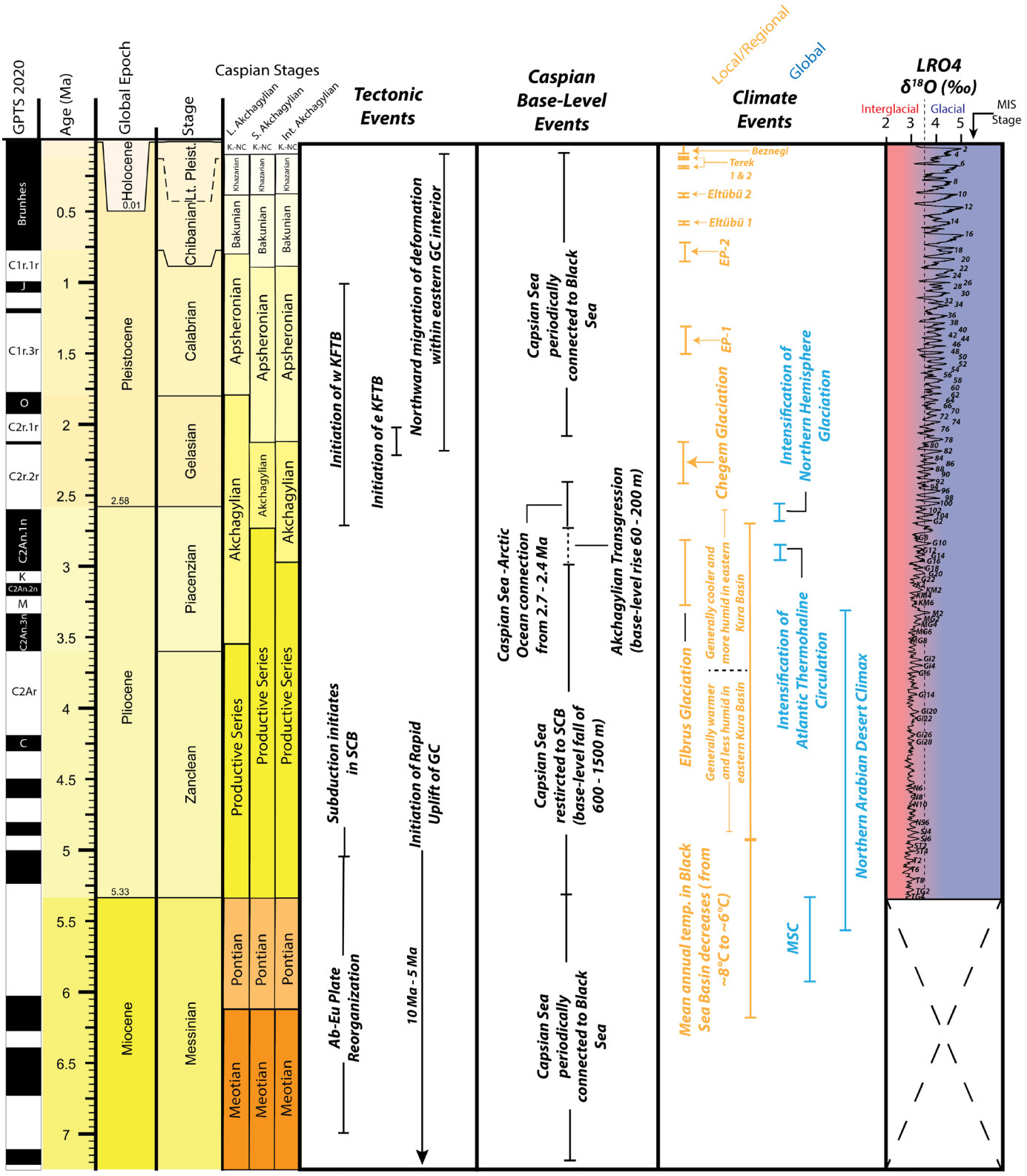

Figure 4 | From left to right: Synthesis of the Caspian Stages and their associated boundaries relative to the GPTS 2020 (from Raffi et al., 2020). A* = Long Akchagylian, B* = Short Akchagylian, C* = Intermediate Akchagylian. Synthesis of the late Cenozoic tectonic, Caspian Sea Base Level, and regional and global climatic events from within and around the Caucasus. LRO4 Stacked $\delta^{18}O$ and associated MIS stage for the Quaternary to Pliocene are derived from the 57 benthic $\delta^{18}O$ records complied and correlated by Lisiecki & Raymo (2005). The age range for Mediterranean Salinity Crisis (MSC) from Hsü et al. (1977) and Krijgsman et al. (1999). The age range for the North Arabian Desert Climax (NADC) from Böhme et al. (2021).

Generally, the refinement of the absolute ages of the Caspian stage boundaries over time within the Caucasus has resulted in several proposed age models with the most variability being the ages in which the Akchagyl stage is defined. At present, three distinct age models exist for the Akchagylian, which we refer to as the "Long Akchagylian", "Intermediate Akchagylian", and "Short Akchagylian". This largely follow previous terminology discussed by Krijgsman et al. (2019) with the "Long Akchagylian" spanning from 3.6 Ma – 1.8 Ma and the "Short Akchagylian" spanning from 2.7 Ma – 2.1 Ma (Figure 4); however, we also modify existing nomenclature for the Akchagylian stage

based on the recent study done by Lazarev et al. (2021). This new magnetostratigraphic work by Lazarev et al. (2021) dates the lower Akchagylian boundary at multiple measured sections (e.g., Kvabebi and Kushkuna) to be 2.95 Ma, with the upper boundary being 2.1 Ma, which we denote as the "Intermediate Akachagylian". This study also follows Lazarev et al. (2021) in considering the "Long Akchagylian" to not be applicable within the GC foreland, after resampling of the Kvabebi section from Agustí et al. (2009) found the Kaena subchron, which has been used to support the "Long Akchagylian" age model, was not present and was then revised to be the upper Gauss chron.

3. Methods

3.1. Paleogeographic Reconstructions

To reflect the position of the reported measured sections more accurately with respect to the GC throughout the late Cenozoic KB and their associated changes in depositional environments, and to ultimately constrain basin response times, we performed a series of paleogeographic reconstructions (Figures 5 – 9). In addition to using stratigraphic information from prior results, we also performed pseudo-palinspastic reconstructions of the positions of each measured section through the timespan of interest. To do this, the KB and surrounding areas were divided into three tectonic blocks based on prior work, with the three blocks being: (1) stable Eurasia (red polygon), (2) LC (yellow polygon) (van Hinsbergen et al., 2020), and (3) Taylsh (green polygon) (van der Boon et al., 2018) (Figures 5 – 9). This process largely follows a similar analysis done by Forte et al. (2022a) to reconstruct the total convergence within the GC. Of note, none of the measured sections lie within any of the blocks defined by the plate reconstructions as these blocks effectively define mountainous regions. Thus, we must "assign" each section to one of the blocks and prescribe its motion via the rotation details for the respective blocks. For this assignment, sections east of the West Caspian Fault are considered to be part of stable Eurasia, and each of the remaining sections were assigned to either the Lesser Caucasus or Taylsh block depending on their location, i.e., sections generally north of the Lesser Caucasus block were assigned to this block. The paleogeographic reconstructions presented in this synthesis were completed using GPlates program (Müller et al., 2018) at a time step of 0.25 Ma over an 8 Ma period. In our reconstructions, stable Eurasia (and measured sections considered to be anchored to stable Eurasia) are held static, and the LC and Taylsh blocks are rotated relative to the Eurasian block's position. Thus, the coordinates in our reconstructions are not strictly accurate as they do not factor in the motion of Eurasia in an absolute reference frame, but the relative positions of the LC and Taylsh blocks and associated measured sections with respect to Eurasia follow published plate reconstructions (e.g., van Hinsbergen et al., 2020). The LC and Taylsh block reconstructions were completed using the rotation files from van Hinsbergen et al. (2020) and van der Boon et al. (2019), respectively. It is important to note that in this reconstruction, we explicitly do not consider what percentage of shortening occurs within the KFTB as opposed to at the rangefront after the initiation of the KFTB, due to a great degree of uncertainty. While we know that this introduces errors into our calculations of distances needed for response time calculations (see Section 4.3), the lack of consistent estimates of total shortening and timing of initiation of individual structures in the KFTB along-strike precludes us from incorporating more realistic and complete palinspastic reconstructions of the measured section locations. The lack of inclusion of shortening within the KFTB is likely more important for periods during and after the Apsheron, i.e., the approximate time for the initiation of the KFTB (Forte et al., 2013b; Lazarev et al., 2019; Sukhishvili et al., 2021). Instead, our results focus on several key time periods, in part dictated by key regional tectonic and/or climatic events.

3.2. Stratigraphic Correlations

To correlate stratigraphy within the KB, we synthesized available published stratigraphic sections throughout the KFTB and neighboring regions. For each section, the presented stratigraphy was redrafted using a consistent format and symbology. The text presented by the original authors for each section was assessed, and when reported, sediment caliber, sedimentary structures, and magnetostratigraphic dating (with uncertainty) were incorporated into the correlations. To ease correlation visualization, the sections presented in this paper are generalized to ensure each section contains similar details. We use published magnetostratigraphic dating, where possible, to directly correlate the measured sections across the KFTB. Magnetostratigraphic dating was compared to the GPTS 2020, with the lower boundary of the Olduvai chron (~1.77 Ma) serving as the hanging line for the majority of the measured sections. When there was no magnetostratigraphic dating for a measured section, adjacent correlations were extrapolated based on the Caspian stage boundary determinations made by the authors. Correlations within the central KFTB were augmented with geochemical correlations of ash beds by Forte et al. (2023).

3.3. Basin Response Time Calculations

Basin response time (T_{eq}) is the estimated time required for a one-dimensional river profile transporting sediment to regain equilibrium in response to a change in the upstream boundary conditions (i.e., tectonic or climate) (Paola et al., 1992) and is approximated with (1):

$$T_{eq} = L^2/v \quad (1)$$

Where v is the diffusivity coefficient [m^2/yr] and L [m] is the basin length, which in this work, is measured from the GC range front to either the approximate position of the axial Kura River (e.g., during the Productive Series) or the

interpreted position of the shoreline within the KB (e.g., during the Akchagyl and Apsheron stages). The original Heller and Paola (1992) study implements basin response time calculations within the fluvially dominated sections of their example basins, and thus we do not extend our basin response time calculations beyond the axial drainage or the KB shoreline throughout the Pleistocene, as it is unclear the extent to which the framework of the diffusional timescale of a 1D river would still be applicable for predominantly subaqueous deposition.

The diffusivity coefficient v is given by (2):

$$v = \frac{-8(q)A\sqrt{C_f}}{C_0(s-1)} \quad (2)$$

Where (q) is the long-term average water supply [m^2/yr] to the basin – roughly equivalent to a length normalized estimate of river discharge, A is a dimensionless coefficient based on the type of fluvial system (i.e., braided vs meandering), C_f is a dimensionless drag coefficient assumed to be 0.01, C_0 is the dimensionless sediment concentration assumed to be 0.6, and s is the specific gravity of the transported sediment, approximated to be quartz with a value of 2.67. All variables listed here follow those from Paola et al. (1992) and their references therein. The only exception is that we attempt to calculate an A value (see discussion below) that better reflects changes in environment and fluvial systems at particular points within the KB.

Here we estimate (q) by incorporating a range of rainfall rates based upon reconstructed late Pleistocene rainfall values from eastern Georgia and Armenia (See Connor & Kvavadze, 2009; Cromartie et al., 2020 for discussion of rainfall value reconstruction methods). From this prior work, we assume the rainfall rate to be 0.3 +/- 0.1 m/yr for a dry environment, and a rainfall rate of 0.5 +/- 0.1 m/yr for a wet environment. Thus, we choose rainfall rates of 0.3 m/yr and 0.5 m/yr for dry and wet climates to be the "representative" climate scenarios for the basin response time calculations. It is worth noting that the KB lacks quantitative paleo-rainfall reconstructions throughout the Plio-Pleistocene, and these rainfall values are extrapolations that are correlative with modern Eurasian steppe environments and thus introduce an aspect of uncertainty into the analysis. Using these rainfall rates listed above, we follow the method employed by Heller and Paola (1992), where (q) is determined by multiplying rainfall rate by the catchment length from the drainage divide to the rangefront. In the GC, the drainage divide has been considered to be mostly static over the timespans of interest in this study and is likely in the same position as the modern drainage divide (Forte et al., 2015b). For our study, the catchment length from the modern drainage divide to the range front in the Eastern GC ranges from 17 km – 22 km, with an average of 18.8 km. This 18.8 km was then used to calculate the long-term water supply, which is then used to calculate the diffusivity component of the basin response time equations (equations 1 and 2). It is important to note that this method assumes that there is no water input from within the basin, and all the water for the fluvial system is being generated from within the GC. While this is clearly a simplification, given the lack of a clear understanding of the drainage network structure within either the northern KB or successor Alazani Basin during the time periods of interest, we feel that this simplification is warranted. For variable A, Paola et al. (1992) assumed values of 0.15 and 1.0 for wholly braided and meandering river systems, respectively. Heller & Paola (1992) and works thereafter do not explicitly address basins that transition from braided to meandering systems along the length of the profile of interest.

To address this issue, an A value between 0.15 and 1.0 was calculated by taking the paleogeographic maps and determining a weighted average value of A, by assessing the proportion of braided to meandering systems along the swath of interest (i.e., a swath that crosses a greater proportion of a meandering environment will have an A value closer to 1.0 and vice versa). As such, we do not formally quantify uncertainty in the A value we use, there is certainly variability in fluvial environments not captured (e.g., a gradational change over distance along a fluvial system) in our reconstructions that impart uncertainty into our response time calculations.

Finally, through the time slices for the Productive Series and Akchagyl stages, we measure L from the approximate position of the modern GC rangefront, which implicitly assumes that the location of the rangefront has remained somewhat static over this period, as does our estimation of L. This embayment of the rangefront position has likely occurred in concert with the initiation of the KFTB (e.g., Forte et al., 2010; Mosar et al., 2010) and thus is mostly relevant for the Apsheronian stage. A variety of results suggest that for the history of the GC development, the modern southeastern GC rangefront has been a locus of shortening and exhumation (e.g., Forte et al., 2015b, 2023). Thus, using the modern rangefront as the origin of our measurements of L is consistent with prior results. During the Apsheronian stage, L, is measured from the inferred position of the KFTB, which is consistent with interpretations that have place the activation of the KFTB during the Apsheronian stage (e.g., Lazarev et al., 2019; Sukhishvili et al., 2021; Forte et al., 2023).

The swaths mentioned above are a series of 8 profiles (#1 – 8 from west to east) that are equally spaced and overlain across paleogeographic maps of the KB for the time slices of interest. The swaths are each oriented NE-SW, to best reflect the general direction of sediment transport coming off the main range and KFTB, assuming sediment transport happened in a unidirectional manner. All calculations for A, L, and all basin response time calculations are performed along these swaths. From the basin response time calculations, done at equal increments along the swath, a series of contours was implemented to show how the basin response time fluctuations in both proximity to the GC and KFTB, as well as to be show along strike varia-

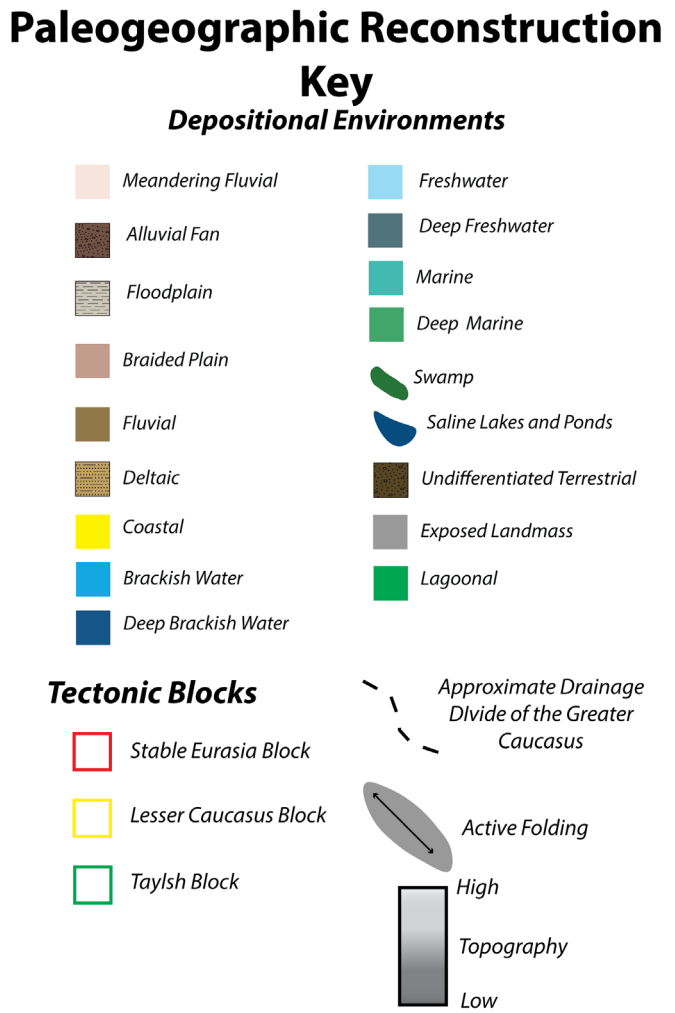

Figure 5 | Key for paleogeographic map depositional environments and tectonic blocks.

tions in basin response time throughout the KB. For these calculations, while we vary L as a function of distance from the rangefront, but follow Heller et al. (1992) in assuming a constant (q) parameter for each swath, i.e., we do not consider that there should be increasing accumulation of discharge at points further into the basin. While obviously a simplification, this in part reflects that there are not sufficiently detailed estimates for drainage network structure within the foreland to accurately reconstruct how discharge would have accumulated downstream within the foreland alluvial rivers. It is also important to note that these are multiple intrabasinal connections between the Caspian Sea and Arctic Ocean (from ~2.75 Ma – 2.45 Ma) and with the Black Sea (from ~2.13 Ma – 2.0 Ma) that can influence Caspian Sea base-level changes. In this scenario, we are opting for a strictly climatically driven (i.e., rainfall induced) base-level change. This is an oversimplifies the Caspian Sea's hydrologic system, but is necessary given the variables dictating the basin response time calculations. Finally, due to the nature of basin response time calculations having to incorporate complex variables that can be difficult to assess, it is best to follow the advice of Paola et al. (1992) and Heller and Paola, (1992), that basin response time values should be viewed as estimations based on assumptions and known values.

4. Results and Discussion

4.1. Late Cenozoic Depositional Environments of the Kura Basin

4.1.1. Productive Series

The Productive Series spans 5.35 Ma – 2.95 Ma based on the new "Intermediate Akchagyl" lower boundary defining the upper Productive Series boundary (Figures 4 and 6). The Productive Series strata is associated with a basin-wide shift in deposition from a shallow brackish water environment to a terrestrial environment that is dominated by fluvial and deltaic processes, depending on the location in KB. The Productive Series is exposed across 6 different measured sections (Figure 10). Specifically, interpretation of the depositional environments for the paleogeographic maps come from along-strike west-to-east measured sections: Vashlovani, Sarica, Hajigabul, Babazanan, Jeirankechmez, and Lokbatan (Figures 6 and 10). In the published measured sections, only the Balakhany, Sabunchi, and Surakhany suites of the Productive Series are predominantly exposed (e.g., Lokbatan, Jeirankechmez, Babazanan, and Sarica) (Vincent et al., 2010; Van Baak et al., 2013; Abdullayev et al., 2018), though the Productive Series suites are not interpreted in all sections (e.g., Forte et al., 2015a) at Vashlovani.

The Vashlovani and Sarica measured sections of Forte et al. (2015a) contain the westernmost exposures of the PS in the KB (Figures 6 and 10). The PS within Vashlovani consists primarily of massive conglomeratic deposits with clasts that range from cobbles to boulder in size (Figure 10; Forte et al., 2015a). Due to the nature of the deposits lacking sedimentary structures, they likely represent either a braid plain or an alluvial fan emanating ≤ 50 km from the southern margin of the eastern GC (Forte et al., 2015a). Forte et al. (2015a) propose that the PS at Vashlovani is likely condensed, precluding PS suite classification. These alluvial fan environments transition to a braid-plane environment towards the axis of the KB. These braided rivers would then feed into the paleo-Kura River that would have been flowing to the east, where incision related to the Caspian Sea regression of -600 – -1500 m resulted in formation of the paleo-Kura Canyon and the paleo-Kura Delta depositing directly into the South Caspian Basin (Reynolds et al., 1998; Hinds et al., 2004; Kroonenberg et al., 2005), however there is no exposure of these features at the surface. The exposures of the PS in Sarica are similar to those in Vashlovani as the PS in Sarica consist primarily of conglomeratic deposits with clasts that range in size from pebble to boulders. The primary difference between the two locations are a greater degree of interbedded coarse sandstones at Vashlovani (Figure 10; Forte et al., 2015a). Geologic mapping by Ali-Zade, (2005) assigned the Productive Series in Sarica to the Balakhany Suite, which represents a low-sinuosity fluvial-floodplain to deltaic environment further east and closer to the Caspian Sea coast (Reynolds et al., 1998; Hinds et al., 2004). While

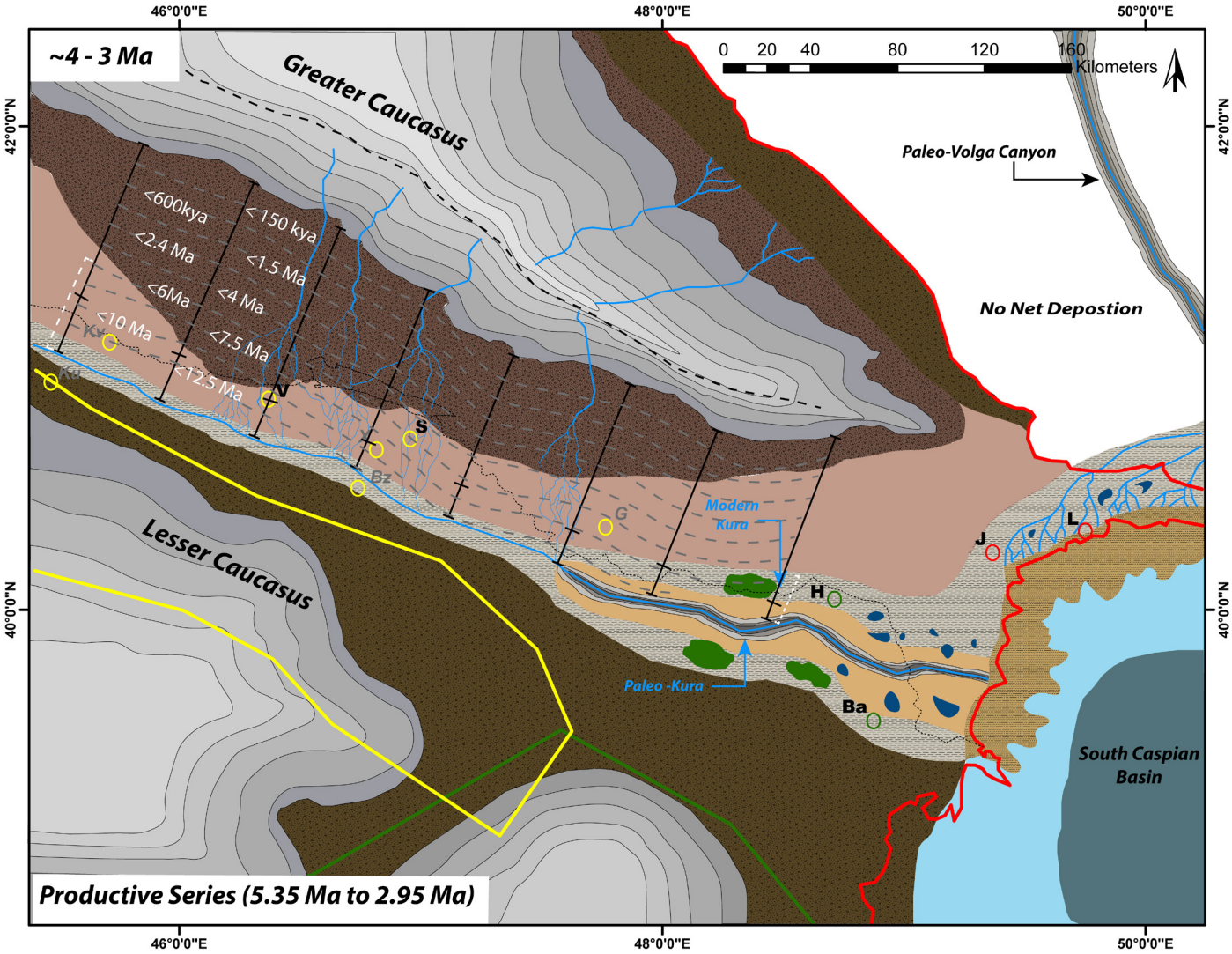

Figure 6 | Paleogeographic map of the Kura Basin, Greater and Lesser Caucasus during the Productive Series at ~4 - 3 Ma. See key (Figure 5) and text for depositional environments. See Figure 5 for symbology discussion. Dashed white brackets show the plausible range of the Kura River. Grey dashed lines are basin response time contours at 10 km intervals.

depositional environment interpretations by Forte et al. (2015a) suggest that the Productive Series in Sarica was a braid-plain environment. The similarity of depositional environments of the PS at both Sarica, Vashlovani, and the eastern edge of the KB indicates that coarse-clastic deposition continued eastwards along the southern margin of the eastern GC. The continuity of these deposits along strike could also be indicative of a continuous system of alluvial fans proximal to the GC along the KB northern margin.

Alluvial deposition likely decreased towards the east, nearing the Caspian Sea, with a transition to more fluvio-deltaic environments (see following discussion on the Productive Series). We cannot exclude that some of these coarse-clastic deposits represent more proximal deposition from initiating KFTB structures, but broadly Productive Series deposition predates the proposed timing of initiation of the KFTB both west (Sukhishvili et al., 2021) and east (Forte et al., 2013b; Lazarev et al., 2019) of these sections.

In the eastern KFTB and KB (e.g., in and around the Lokbatan, Jeirankechmez, and Babazanan sections), Productive Series deposits are finer grained and primarily deltaic in origin (e.g., Vincent et al., 2010; Van Baak et al., 2013) in contrast to the exposures in the western Vashlovani and Sarica sections. Throughout the Productive Series stage, prominent deltaic systems were present along the western, northern, and eastern margins of the South Caspian Basin as the paleo-Kura Delta, paleo-Volga Delta, and paleo-Amu Darya, respectively (Reynolds et al., 1998; Hinds et al., 2004; Kroonenberg et al., 2005; Vincent et al., 2010; Van Baak et al., 2013, 2019), with the eastern sections largely reflecting this history.

The Hajigabul section, first presented by Lazarev et al. (2019), is ~180 km east of the Sarica measured section. The Productive Series in the Hajigabul section consists of fine to coarse sands that have interbedded claystones and siltstones (Figures 6 and 10; Lazarev et al., 2019). A lack of detailed description of sedimentary structures from the Productive Series in Hajigabul precludes an exact interpretation of the type of fluvial environment during this period. Based on the presence of floodplain deposits that

tend to be pedogenically altered (Lazarev et al., 2019), a stable sub-aerial environment persisted along the axial Kura River that was likely flowing through or near the approximate area between 4 – 3 Ma. Further east in the KB, exposures of the Surakhany Suite of the Productive Series occur in the Babazanan section (Vincent et al., 2010). The Productive Series at Babazanan consists primarily of fine sand with interbedded clay and siltstones (Vincent et al., 2010; Van Baak et al., 2015). East of Hajigabul, on the Apsheron Peninsula, is the Jeirankechmez section. The upper PS in Jeirankechmez predominantly consists of finer-grained sandstones with a greater concentration of silt and mud (Richards et al., 2018; Van Baak et al., 2019). The Lokbatan section along the eastern Apsheron Peninsula and has been the focus of multiple stratigraphic and palynological studies, often used as an analogue for offshore equivalents of the Productive Series in the South Caspian Basin (e.g., Reynolds et al., 1998; Hinds et al., 2004; Van Baak et al., 2013; Hoyle et al., 2018; Richards et al., 2021). The Productive Series in Lokbatan primarily consists of interbedded cross-laminated sandstones with some symmetric ripples, silt, and claystones (Van Baak et al., 2013).

In summary, the PS from 4 – 3 Ma records primarily terrestrial depositional environments along the southern margin of the GC. First-order variations in depositional environment interpretations consistently show that the more western and central portions (e.g., Vashlovani and Sarica) of the KB during this time are dominated by alluvial fan and braided fluvial environments. During this time, the rapidly uplifting GC likely supplied ample coarse sediment that could explain the development of braided-fluvial environments and alluvial fan deposition ~50 km into the KB. Alluvial fan and braided-fluvial environments likely persisted along the northern and southern margins of the GC, while further east, there is a transition to predominantly fluvial-floodplain and fluvio-deltaic depositional environments. Some of the floodplains in portions of the KB were also periodically inundated, resulting in swamp formation and isolated lacustrine environments (Vincent et al., 2010). The lacustrine environments were likely hypersaline, owing to periodic drying of the isolated lakes within the floodplains of both the paleo-Kura and along the paleo-Volga Delta (Vincent et al., 2010).

4.1.2. Akchagyl

The Akchagyl stage (2.95 Ma - 2.1 Ma) highstand deposits are found throughout the KB and KFTB, ranging from more western sections, e.g., Kushkuna, Kvabebi, Vashlovani, Sarica, and Göychay to the eastern sections of Hajigabul, Babazanan, Jeirankechmez, and Lokbatan. The following sections are presented from west to east (Figures 7 and 8).

In the 300 m thick Kushkuna section by Ali-Zade et al. (1972) and Jorissen (2020), the upper 240 m of this section consists of mudstones and siltstones that coarsen upwards into fine-grained sandstones attributed to the Akchagylian, with age control from Jorissen (2020) and Lazarev et al. (2021). The Akchagyl starting at ~2.95 Ma in Kushkuna represents the arrival of a freshwater flooding event that inundated the western extent of the Kura Basin. From 60 m – 235 m, the Akchagyl at Kushkuna was dominated by a lagoonal environment with a predominantly muddy coastline (Jorissen, 2020). From ~ 90 m to 210 m, fresh and brackish water mollusks are found at points throughout the Akchagylian deposits, supporting freshwater inundating far into the western extent of the Kura Basin (Jorissen, 2020). At ~2.6 Ma, Jorissen (2020) notes a significant change in the depositional environment at Kushkuna where the predominantly lagoonal environment is replaced by a floodplain environment with a meandering fluvial setting. This transition in depositional environments is indicative of a regression of the Caspian waters within the western Kura Basin by ~2.6 Ma.

In Kvabebi, first described by Agustí et al. (2009) and then by Jorissen (2020), the Akchagylian is 260 m thick and predominantly consists of siltstones with some interbedded fine to coarse sandstones. The primary lithological difference between Kushkuna and Kvabebi is the presence of three ash beds in the middle portions of the section between 128 – 136 m at Kvabebi. The ash bed at 129 m was dated by Lazarev et al. (2021) via $^{40}Ar/^{39}Ar$ to be 2.86 Ma and is in good agreement with the magnetostratigraphic dating by Jorissen (2020) and Lazarev et al. (2021).

At Kvabebi, based on magnetostratigraphic dating done by Jorissen (2020) and Lazarev et al. (2021), radiometric dating of an ash bed by Lazarev et al. (2021), and stratigraphic correlation of storm deposits by Jorissen (2020), the lower 160 m of the section is correlative to the Gauss chron. The lower 10 m of the Kvabebi section is interpreted as a nearshore environment with a significant amount of silt and mud components (Jorissen, 2020). From 10 m – 170 m, the Kvabebi section transitions to a lagoonal and floodplain environment with some fluvial input. From 0 m – 170 m, there are some brackish to freshwater mollusks which, like in Kushkuna, support freshwater inundation into the western Kura Basin. Like Kushkuna, the Kvabebi section also shows distinct change in depositional environment, with the disappearance of brackish and freshwater mollusks, and a shift to a predominantly braided-fluvial environment (Jorissen, 2020). The change in depositional environments from low-energy floodplain and lagoonal settings to terrestrial high-energy fluvial systems is correlative to a near contemporaneous regression of the Caspian waters within the western Kura Basin (Jorissen, 2020; Lazarev et al., 2021).

In the Vashlovani section, the Akchagylian stage is ~480 m thick and consists of silt and claystone with some interbedded fine to medium-grained sandstones (Figures 7, 8 and 10). The age of the lower boundary of the Akchagylian within the Vashlovani section lacks chronologic control due to a lack of dateable ash beds, magnetostratigraphic dating, or stage indicative biostratigraphic markers. This

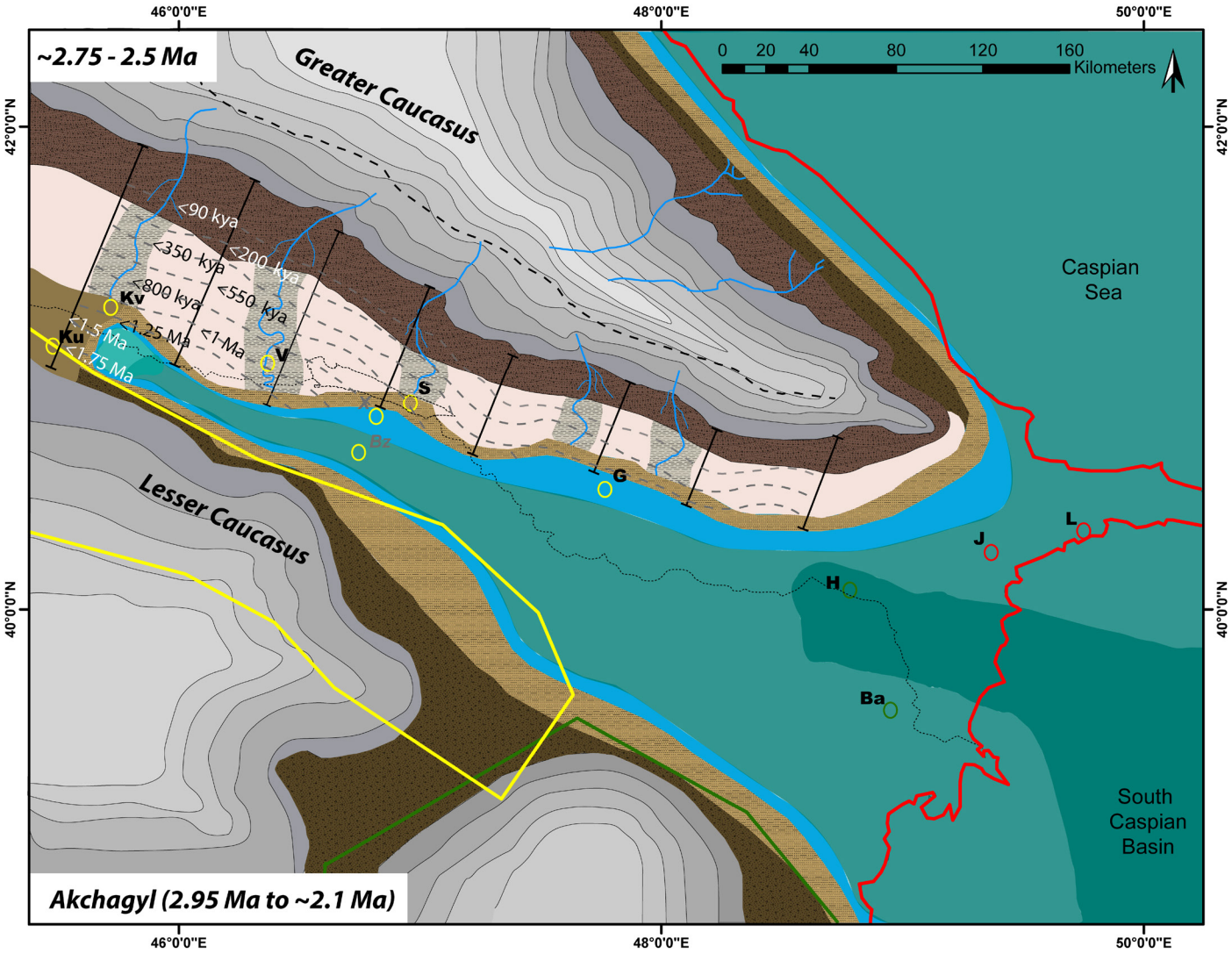

Figure 7 | Paleogeographic map of the Kura Basin, Greater and Lesser Caucasus during the Akchagylian at ~2.75 – 2.5 Ma. See key (Figure 5) and text for depositional environments. See Figure 5 for symbology discussion. Grey dashed lines are basin response time contours at 10 km intervals.

precludes precise correlation with the adjacent measured sections. In Vashlovani, the Akchagylian sediments were deposited in a meandering fluvial environment that fed into a brackish water lacustrine system that periodically inundated the meandering fluvial floodplains (Forte et al., 2015a). Further east, a ~700 m thick section of the Akchagylian stage is exposed within the Sarica section. Lithologically, the Akchagylian at Sarica consists of mostly siltstones and claystones, with a significant interbedded coarse sand and gravel component throughout. Like Vashlovani, a meandering fluvial depositional environment was present along with a broad floodplain, periodically inundated by a brackish lacustrine system. The coarse-grained sand, silt, and claystone deposits provide evidence for Gilbert-type deltas developing along the margins of the brackish Caspian Lake (Forte et al., 2015a). Based on the proximity between the Vashlovani and Sarica sections, it is likely that a Gilbert-type deltaic system persisted along the northern margin of the intruding Caspian Sea within the KB. The presence of a Gilbert-type delta system and its sedimentary architecture results from an increase in sediment supply sourced from the rapidly uplifting GC and the southward progradation of deltaic facies associated with the possible activation of the KFTB (Forte et al., 2015a).

The Göychay section, reported by Forte et al. (2013b) and Lazarev et al. (2019), exposes ~700 – 800 m of the Akchagylian stage. The Akchagylian stage at Göychay consists primarily of mudstones and siltstones with few interbedded fine to coarse-grained sandstones. The Akchagylian deposits in Göychay, based upon magnetostratigraphic dating and structural analysis spans from ~2.6 Ma to 2.1 Ma (Forte et al., 2013b; Lazarev et al., 2019). The lowest Akchagylian (~2.6 – 2.5 Ma) exposures of mudstones and siltstones indicate a distal to open-water mesohaline environment; these deposits are replaced by freshwater prodeltaic mudstones (~2.5 Ma – 2.4 Ma). This series of prodeltaic mudstones and siltstones is correlative with deltaic facies found further west in the Sarica and Vashlovani sections by Forte et al. (2015a) and the terrestrial transition in Kvabebi and Kushkuna by Lazarev et al. (2021). Lazarev et al. (2019) link this transition to prodeltaic deposition to the activation of the eastern KFTB between 2.2 – 2.0 Ma, resulting in the progradation of delta fronts due to a forced base-level regression. The overall timing

of the transition to deltaic/terrestrial environments seen throughout the sections discussed above is indicative of a nearly synchronous, along strike activation of the KFTB from west to east, as proposed by Sukhishvili et al. (2021) and Forte et al. (2023).

The Hajigabul section, reported by Lazarev et al. (2019), exposes ~370 m of Akchagylian stage deposits. The base Akchagylian stage here consists of mostly blue mudstones with some interbedded siltstones, with the top of the stage consisting of a transition to medium-grained, cross-bedded sandstones. Lazarev et al. (2019) note that the Akchagylian deposits at Hajigabul are impoverished in microfauna. Lazarev et al. (2019) interpret the low concentrations of microfauna at Hajigabul to reflect water depths that were likely too deep to preserve microfauna between 2.6 Ma – 2.1 Ma, making an exact paleoenvironmental interpretation difficult. As such, this suggests the sediment of the Akchagylian stage at Hajigabul was deposited distally, in a deeper portion of the KB further from the KFTB.

The Babazanan section, as reported by Vincent et al. (2010), exposes ~95 m of the basal Akchagylian stage sediments. Here the Akchagylian stage lithologically consists of mostly mudstones and siltstones, with several ash beds found near the base (Vincent et al., 2010). Due to its location, the Babazanan is both distal from the GC range front and the KFTB during the Pleistocene, and would have likely been inundated for much, or all, of the Akchagylian stage, containing both distal freshwater to brackish water depositional environments.

The Jeirankechmez section, reported by Richards et al. (2018) and Van Baak et al. (2019), exposes ~315 m of Akchagylian stage. The Akchagylian stage in the Jeirankechmez section lithologically consists of mostly grey and tan-coloured claystones and siltstones with some fine to medium-grained sandstones. At Jeirankechmez, the Akchagylian transgression occurs at 770 m, marked by the appearance of brackish-water microfauna that persists until 790 m (Richards et al., 2018). Benthic marine foraminifera (e.g., *Cibicides Cassidulina*) first appear at 790 m in the Jeirankechmez section (Richards et al., 2018), marking the appearance of marine conditions within the eastern KB that post-dates fresh to brackish water flooding throughout the foreland. Along with magnetostratigraphy, the lower portions of the Akchagylian stage at Jeirankechmez, like Babazanan, have multiple ash layers found near the base. The ages of these ash beds are constrained by biotite $^{40}Ar/^{39}Ar$ dating, with two of the lowest ash beds at 779 m and 789 m yielding ages of 2.68 +/- 0.03 Ma and 2.65 +/-0.04 Ma, respectively (Van Baak et al., 2019). Based on radiometric dating, magnetostratigraphic dating, and biostratigraphic markers, the lower boundary of the Akchagyl in the Jeirankechmez is correlative with an age of ~2.75 Ma, which agrees with the proposed age of the Akchagylian Marine Incursion (AMI) by Van Baak et al. (2019). Lazarev et al. (2021) and Hoyle et al. (2021) then distinguish that the Akchagylian transgression pre-dates the AMI at 2.95 Ma, with the transgression being followed by a transition to brackish conditions which give way to marine conditions sourced from the Arctic Ocean. The upper Akchagylian at Jeirankechmez does not significantly differ lithologically and biostratigraphically from the lower Akchagylian. The primary difference between the upper and lower Akchagylian is that predominantly brackish water dinoflagellate cysts mark the upper portions of the stage (e.g., *Bitectatodinium*) (Richards et al., 2018). The presence of brackish water dinoflagellates does not fluctuate significantly in the more distal portions of the KB post 2.45 Ma, but throughout most of the KB there is a disappearance of marine fauna, and subsequent consistent freshwater and brackish water fauna found near the basin edges (Richards et al., 2018; Lazarev et al., 2019; Van Baak et al., 2019; Hoyle et al., 2021). These trends indicate that the Arctic Ocean source for the marine microfossils within the Caspian had likely been cut off by 2.45 Ma by isostatic rebound within the Volga's catchment, resulting in the Caspian Lake gradually becoming more brackish-oligohaline, similar to most of the inundated KB at this time (Richards et al., 2018, 2021; Van Baak et al., 2019 Lazarev et al., 2021).

On the Apsheron Peninsula, the Lokbatan section presented in multiple studies (e.g., Reynolds et al., 1998; Hinds et al., 2004; Vincent et al., 2010; Van Baak et al., 2013; Richards et al., 2021), exposes ~120 m of Akchagylian stage sediments. These Akchagylian sediments consist primarily of brown–grey clays and siltstones with multiple thin ash beds throughout the exposure. Hoyle et al. (2021) found the lowermost Akchagylian sediments are indicative of deposition within a freshwater environment based on the abundance of freshwater algae (e.g., *Pediastrum*). Post 2.75 Ma, Hoyle et al. (2021) observed the replacement of freshwater algae by the marine dinocyst *Operculodinium centrocarpum*. Chronological constraint of this change comes from $^{40}Ar/^{39}Ar$ dating from ashes at Lokbatan by Hoyle et al. (2020) and by Van Baak et al. (2019) at Jeirankechmez, which dated a lower ash bed at 528 m and 779 m to be 2.73 +/- 0.09 Ma and 2.68 +/-0.03 Ma, respectively. This results in the lower ash beds of the Lokbatan section being correlative with the initiation of the AMI between ~2.75 Ma – 2.7 Ma (Van Baak et al., 2019; Lazarev et al., 2021). The upper Akchagylian deposits in Lokbatan are similar lithologically to the basal portion, as they predominantly consist of blue-grey mudstones and siltstones. Hoyle et al. (2021) determined that the upper Akchagylian deposits in Lokbatan exhibit a decline in the marine palynomorphs and an increase in the abundance of brackish dinocysts (e.g., *Pyxidinopsis* and endemic *Spiniferites crusciformis*). The result is consistent with similar indications in other measured sections in the eastern KB (proximal to the Caspian Sea) that all record a decrease in the salinity within the Akchagylian stage

In summary, the Akchagylian stage throughout the KB represents both basin-wide and regional flooding events

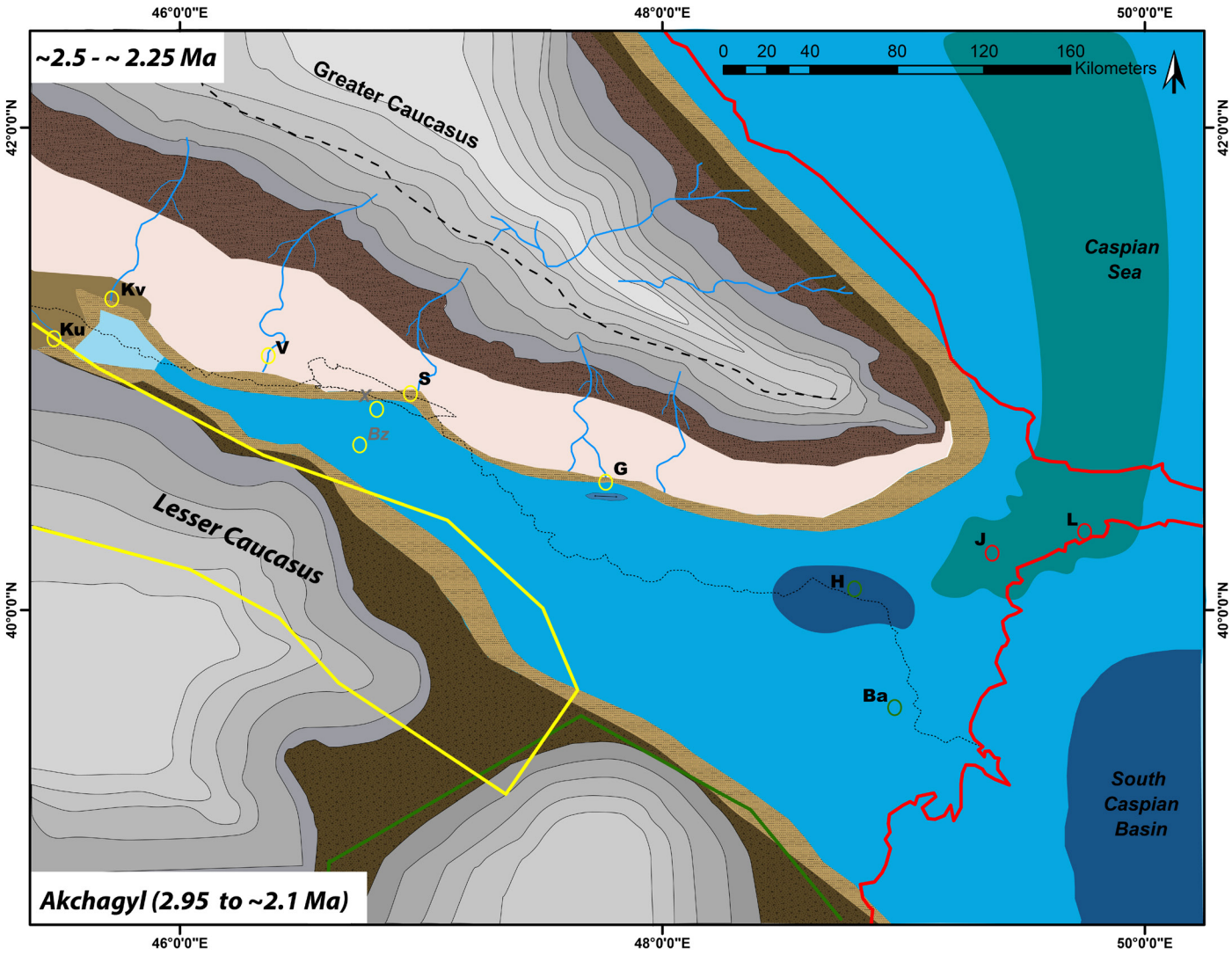

Figure 8 | Paleogeographic map of the Kura Basin, Greater and Lesser Caucasus during the Akchagylian at ~2.5 – 2.25 Ma. See key (Figure 5) and text for depositional environments. See Figure 5 for symbology discussion.

that inundated nearly the entire area of modern-day Azerbaijan and eastern Georgia, and in return, represents a shortening of the depositional system within the northern KB, i.e., a decrease in the distance between the GC rangefront and the Caspian shoreline (Figures 7 and 8). The onset of a positive water budget in the circum-Caspian Basin region is proposed by Lazarev et al. (2021) as the possible mechanism for the large transgression of the Caspian Lake at ~2.95 Ma. This mechanism could explain the presence of freshwater palynomorphs found near the base of the Akchagylian stage at both Jeirankechmez and the Lokbatan. The timing of this expansion is also generally correlative with an increase in sea surface temperatures and the resulting intensification of the Atlantic Thermohaline Circulation and could explain an increase in precipitation in the Caspian Lake drainage basins (Bartoli et al., 2005; Lazarev et al., 2021; Vasiliev et al., 2022). The Akchagylian stage in the KB then transitioned to a marine-dominated environment from ~2.7 Ma – 2.4 Ma, with marine water likely sourced from the Arctic Ocean (Figures 7 and 8; Van Baak et al., 2013, 2019; Richards et al., 2018; Krijgsman et al., 2019; Hoyle et al., 2021; Lazarev et al., 2021). The severing of the marine connection occurred by ~2.4 Ma, during and after which the Caspian Lake transitioned to a lower salinity environment with riverine input into the Caspian Basin (Lazarev et al., 2019; Hoyle et al., 2021). Akchagylian sediments during this time reflect relatively distal deposition of fine-grained siltstones and mudstones with the occasional interbedded fine to medium-grained sandstone. The result is that many of the Akchagylian stage exposures are condensed relative to Productive Series or Apsheronian stage deposits. The gradational changes from freshwater to marine to brackish water environments that share many palynological and microfossil assemblages continues up section as many of the upper Akchagylian microfossil and palynological assemblages carry across the lower boundary of the Apsheronian stage, which makes it difficult to locate the exact Akchagyl-Apsheronian boundary within the KB and KFTB.

4.1.3. Apsheron

The Apsheronian stage (2.13 Ma – 0.85 Ma) exposures can be found throughout the KB, with the westernmost exposure considered here occurring in the Xocashen section presented by Forte (2012) and Van Baak et al. (2013) (Figure 9). Further west, the upper portion of

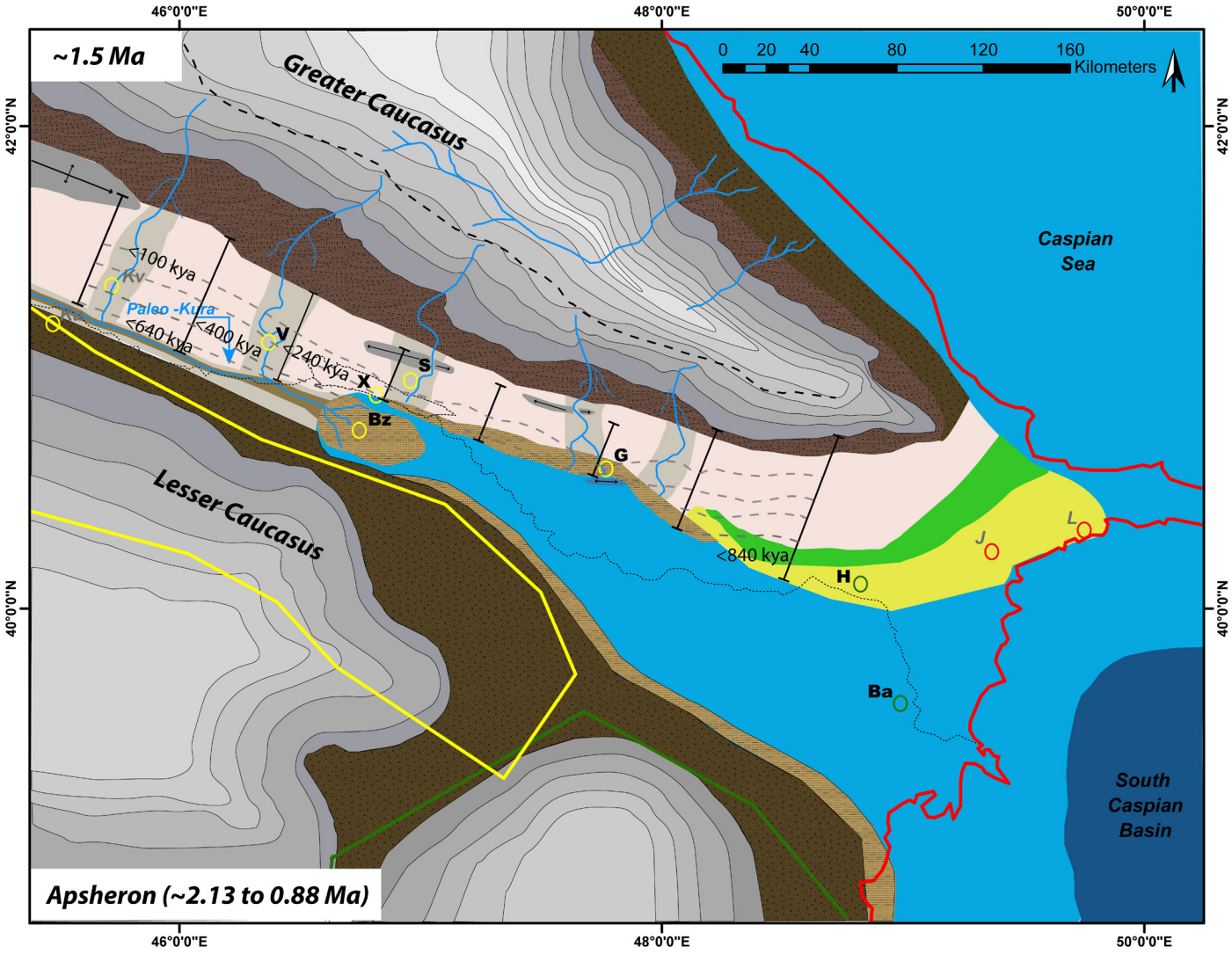

Figure 9 | Paleogeographic map of the Kura Basin, Greater and Lesser Caucasus during the Apsheronian at ~1.5 Ma. See key (Figure 5) and text for depositional environments. See Figure 5 for symbology discussion. Grey dashed lines are basin response time contours spaced at 10 km intervals.

Vashlovani may also expose the lower Apsheron, but as the exact boundary between the Akchagyl and Apsheron is unclear in this section we do not use the exposure in Vashlovani in our synthesis. The Apsheronian of the Xocashen section consists primarily of ~ 600 m of unlaminated siltstones and claystones with some small channels preserved as <1 m thick sandstone intervals, instances of reworked shells in the coarser fractions, and a ~1.5 m thick ash bed at 475 m (Forte, 2012). A study by Van Baak et al. (2013) noted the presence of lacustrine freshwater ostracods (e.g., genus *Ilyocypris*) in the lower 570 meters of the exposed Apsheronian strata, but no age-indicative species present within the section. Even though no age indicative Apsheronian fauna are found, Van Baak et al. (2013) notes a transition from freshwater to brackish water ostracod assemblages (e.g., Ammicythere pediformis, Ammicythere cymbula, and Loxoconcha babazanica) above 570 meters. The Apsheronian stage at Xocashen represents a marginal lacustrine environment that initially consisted of freshwater conditions, possibly related to greater riverine input or a climatic shift (e.g., Van Baak et al., 2013) within the western portion of the Caspian Lake, which was then replaced by brackish water conditions like the modern-day Caspian and Black Seas (Figure. 9). A lack of widespread and thick fluvial deposits could indicate the coastline had undergone only minor fluctuations throughout the Apsheronian transgressions.

The Bozdagh section exposes ~1 km of Apsheronian stage strata along the backlimb of the Bozdagh fold, south of the Xocashen section and across the Mingachevir Reservoir (Forte, 2012). Neither the basal Akchagylian-Apsheronian or overlying Apsheronian-Bakunian boundary are observed in the Bozdagh section, so this exposure only represents a portion of the Apsheron stage at this location. Stratigraphically, the Apsheronian at Bozdagh consists of predominantly grey to blue claystones and siltstones, with periodic cross-stratified sandstones with mud-clast conglomerates, and sporadic mammalian and terrestrial (e.g., tree stumps) fossils (Figures 9 and 10; Forte, 2012). Ostracod assemblages within the Apsheronian stage, in this section, are consistent with deposition in a brackish water environment (e.g., *Ammonia beccari*), with salinity values like that of the modern-day Black Sea, displaying occasional instances of freshwater ostracod assemblages (e.g., *Ilyocypris bradyi* and *Ilyocypris gibba*) (Forte, 2012).

Forte (2012) interprets the unlaminated siltstones and claystones with plant debris, coupled with the ostracod assemblages, to reflect a marginal lacustrine depositional environment that was proximal to the coast and sediment source. The cross-stratified sandstones with mud-clast conglomerates represent a fluvio-deltaic environment undergoing active lobe switching that would have been depositing sediment along the margins of the Caspian Lake, and potentially representing a delta of the paleo-Kura River (Forte, 2012).

The Sarica section exposes ~1.3 km of Apsheronian stage sediments consisting of unlaminated siltstones and claystones that transition into coarse-grained sandstones and gravels (Forte et al., 2015a). From ~900 m – 2200 m, the Apsheronian stage strata primarily consist of a coarsening upwards trend, with the middle portions of the Sarica section consisting of cross-stratified, coarse-grained sandstone with gravel, that transitions into massive gravel conglomerates (Forte et al., 2015a). The unlaminated siltstone and claystone deposits of the lower Apsheronian at Sarica are interpreted by Forte et al. (2015a) to reflect a floodplain environment with occasional overbank deposition and inundation of the KB. Although the Sarica section lacks a detailed record of the possible microfossil assemblages, the presence of both gastropods and bivalves found throughout the unlaminated mudstones supports a floodplain that is periodically inundated via the Caspian Lake. Forte et al. (2015a) interpret the laterally discontinuous, cross-stratified, coarse-grained sandstones to represent an anastomosing to braided fluvial-deltaic environment. The uppermost Apsheronian thick gravel conglomerates likely indicate the presence of alluvial fan progradation over the fluvial environment KB (Forte et al., 2015a). The Apsheronian stage at Sarica is representative of a long-term coarsening upwards trend that shows the progradation of a fluvial-deltaic system within central portions of the KB, that was overstepped by the progradation of alluvial fans further into the basin (Forte et al., 2015a). The source of these gravels during the Apsheronian likely reflects a mixture of continued uplift of the GC and/or initiation of the KFTB and segmentation of the KB (Forte et al., 2010, 2013b, 2015a; Sukhishvili et al., 2021).

The Apsheronian stage in the Göychay section is ~1500 m thick, spanning ~2.1 Ma – 1.13 Ma, and was reported initially by Forte et al. (2013b) and then later by Lazarev et al. (2019). The Apsheronian at Göychay consists primarily of siltstones, coarse-grained sandstones, and cobble conglomerates near the top of the exposed section. The upper Akchagylian – lower Apsheronian contact is gradational, lacks any definitive lithologic changes between the stage boundaries, and is generally marked by the disappearance of marine foraminifera *Ammonia* sp. and brackish ostracods (e.g., *Cyprideis torosa* and *Tyrhenocythere azerbaijanica*), resulting in a predominantly barren section with rare freshwater ostracods *Candona* sp. (Lazarev et al., 2019). These lacustrine conditions that post-date the Akchagyl – Apsheronian persist from ~2.1 Ma to ~1.85 Ma, with the final appearance of the Apsheronian mollusk fauna occurring at 1018 m in the Göychay section (Lazarev et al., 2019). The Apsheronian strata above the Akchagylian-Apsheronian boundary show a coarsening upwards trend from siltstones with periodic coarse-grained sandstones and gravels (Forte et al., 2013b; Lazarev et al.,2019). This coarsening upward sequence is thought to represent periodic underflows of dense sediment plumes into the Caspian Lake, with the overall increase in grain size above the Akchagylian – Apsheronian boundary indicating the likely source for the sediment is more proximal to the Caspian Lake margin (Lazarev et al., 2019). This increase in grain size is correlative with observations made throughout the Apsheronian strata found throughout the western–central KB, and is correlative with the timing of the initiation of deformation along the KFTB and the presence of fluvio- deltaic facies (Forte et al., 2010, 2013b, 2015a; Lazarev et al., 2019). The uppermost Apsheronian deposits are composed of coarse-grained sandstones with preserved channels and gravel conglomerates, and interbedded siltstone. This is interpreted by Lazarev et al. (2019) as the Ushtal Suite, a unique subset of the Apsheronian stage that consists of alluvial deposits. This transition from a fluvio-deltaic to lacustrine depositional environment to a solely terrestrial fluvial-floodplain is marked by the appearance of mollusk fauna (e.g., *Abida* sp., *Chondrula* sp., *Gyraulus* sp.) (Lazarev et al., 2019). The transition from a predominantly lacustrine -fluvio-deltaic to strictly fluvial depositional environment is consistent with an increase in sediment supply, induced by tectonism in the main range and within the foreland basin (e.g., Forte et al., 2013b, 2015a). Forte et al. (2015a) interpret this as a tectonic driver, although they acknowledge climate (e.g., glaciation-induced sediment flux) could produce the coarsening upwards trend seen throughout the Vashlovani, Sarica, and could be a possible mechanism for trends seen further east in Göychay. In general, from Xocashen, Bozdagh, Sarica, and Göychay measured sections, the fine-grained deposits of the lower Apsheronian are replaced by fluvio-deltaic coarse-grained sandstones and cobble conglomerates. This study favors the interpretation that an increase in grain size and appearance of cobble conglomerates is likely the result of a mixture between the rapid uplift of the GC since 5 – 10 Ma, and/or the southward progradation of the deformation front into the KB resulted in the activation of the eastern KFTB at ~2.2 – 2.0 Ma, leading to the progradation of the gravel front and deltaic facies deeper into the KB (Forte et al., 2010, 2013b, 2015a, 2015b, 2022a; Lazarev et al., 2019; Sukhishvili et al., 2021).

The Hajigabul section exposes ~1 km of Apsheronian stage sediments and was initially described by Jorissen et al. (2020). The Apsheronian at Hajigabul represents a series of ~20 regressive trends (Jorissen et al., 2020). Each regression occurs at a ~50 – 100 m interval, and consists of multiple facies defined by Jorissen et al. (2020). The lower component to each facies consists of horizontally

laminated siltstones that then transition to fine – medium grained cross-bedded sandstones, that are overlain by fine to very-coarse grained sandstones with noted shell stringers, which are in turn overlain by organic rich mudstones with some freshwater fauna and pedogenic features (Jorissen et al., 2020). These facies are considered to represent regressive packages showing the transition from a more distal, offshore environment, to shoreface setting, to foreshore and backshore environments, that then transitions into lagoonal and floodplain environments at the top (Jorissen et al., 2020). Lazarev et al. (2019) note that the Akchagylian – Apsheronian boundary at Hajigabul occurs at the first appearance of oligohaline mollusks *Monodacna* sp. and *Apsheronica propinqua* and ostracod T*yrrhenocythere azerbaijanica*. These macro- and micro-fauna are indicative of a coastal to nearshore depositional environment. There are possibly differing mechanisms for the arrival of coarse-grained sands during the Apsheronian. A similar tectonic mechanism like the ones recorded in Göychay is a plausible reason for the increased coarse-grained sediment flux, and ultimately, the progradation of coarse-grained transitional environments in Hajigabul. A tectonic mechanism is not favored by Lazarev et al. (2019), who instead associates the appearance of coarse-grained sediment as the result of a basin-wide regression of the Caspian Lake during the Apsheronian and cannot be due to a discrete structure or wholly tectonic explanation. Recent works by Jorissen et al. (2020) and Hoyle et al. (2020) have found that the sedimentary successions within the eastern Kura Basin at sections such as Lokbatan and Hajigabul reflect changes in obliquity on a 41-kya timescale.

The Apsheronian stage at the Babazanan section was initially presented by Vincent et al. (2010) and Van Baak (2015). The study by Vincent et al. (2010) focuses on the Surakhany suite of the Productive Series that makes up the bulk of the lower Babazanan section and does not provide any discussion on the Apsheronian strata. Van Baak (2015) originally interpreted the Babazanan section to mainly consist of the Productive Series and Akchagylian stage sediments, with only the uppermost ~100 m made of Apsheronian stage sediments. In a recent study by Lazarev et al. (2021), the Akchagylian stage is reported as being ~60 m thick, resulting in the lower boundary of the Apsheronian stage at Babazanan occurring at 530 m. This synthesis will use Lazarev et al. (2021) to assess the Babazanan stage boundaries and correlations between the adjacent sections within the KB. A lack of detailed stratigraphic assessment of the Apsheronian stage sediments at Babazanan hampers an accurate evaluation of paleo-depositional environments. Based on the position of the Babazanan section within the KB during this time (~2.1 Ma – 0.88 Ma), proximity to the modern-day Caspian Sea, and the depositional environment interpretations, the Apsheronian at Babazanan likely reflects a distal open-water mesohaline environment.

The Jeirankechmez section, reported initially by Richards et al. (2018) and then later Van Baak et al. (2019), is proximal to the modern-day Caspian Sea. Apsheronian exposure is between 500 m – 700 m with no clear lithologic or biostratigraphic markers to precisely pinpoint the lower stage boundary (Lazarev et al., 2019; Van Baak et al., 2019). The Apsheronian strata at Jeirankechmez are a mixture of light brown-grey marls, siltstones, and claystones (Richards et al., 2018). A lack of lithologic and sedimentary structure descriptions presented by Richards et al. (2018) and Van Baak et al. (2019) precludes any distinct lithologic component to depositional environment interpretations and is dependent upon microfossil and palynological assemblages. The Apsheronian at Jeirankechmez is marked by an increase in the number of ostracod species coupled with indicative Apsheronian ostracods *Tyrhenocythere azerbaijanica*, and *Cytherisa bogatschovi* found in the upper portion of the section, confirming deposition during the Apsheronian stage (Richards et al., 2018). Based upon the presence of brackish water ostracods and the very-fine-grained nature of the Apsheronian lithologies, deposition occurred in a lacustrine environment with brackish water conditions, likely the Caspian Lake that persisted in the region post-Akchagylian.

Northeast of Jeirankechmez is the Lokbatan section exposed on the Apsheron Peninsula along the coast of the modern-day Caspian Sea. This section was reported initially by Van Baak et al. (2013), who interpreted that ~190 m of Apsheronian strata is exposed at Lokbatan. Like Jeirankechmez, Van Baak et al. (2013) noted that there is no distinct lithologic boundary between the Akchagylian and Apsheronian stages and is defined based on micropaleontological assemblages. The sediment of the Apsheronian at Lokbatan consists predominantly of laminated blue to brownish-grey silty-claystone with occurrences of ferruginous layers and iron concretions (Van Baak et al., 2013). The microfauna at Lokbatan, like in Jeirankechmez, show no distinct change across the Akchagylian – Apsheronian boundary, with the boundary being placed at a marked increase in ostracod species *Tyrhenocythere donetziensis* and *Tyrhenocythere pontica* (Van Baak et al., 2013).

Based on the presence of laminated slitstone and claystone and the increase in ostracod of Tyrhenocythere species, it is indicative of a quiescent brackish lacustrine environment (Van Baak et al., 2013). This reflects the Caspian Lake having inundated the Apsheron Peninsula during the mid-Pleistocene.

4.2. Kura Basin Stratigraphic Correlations

Because of the extreme stratigraphic heterogeneity within the KB, direct lithologic correlations across key Caspian stage boundaries are valid only over short distances within the KB. This synthesis instead primarily uses published magnetostratigraphic dating across KB for the presented measured sections, and when possible, are used in conjunction with geochemically correlated ash beds

(Figure 10). Our magnetostratigraphic correlations are largely consistent with the most recent work by Lazarev et al. (2019, 2021) and Van Baak et al. (2013, 2015, 2019). Magnetostratigraphic dating can allow for direct correlation of most of the measured sections in both the KB and KFTB. In the absence of either magnetostratigraphy or ash horizons (e.g., Sarica, Vashlovani), we correlate based on published or inferred ages of portions of sections from prior mapping by Ali Zade (2005) and Forte et al. (2015a).

The upper boundary of the Olduvai chron (1.77 Ma) acts as the primary hanging line upon which all the stratigraphic correlations are made because of its presence in 5 out of 11 presented sections, allowing for decent correlation of the Apsheron stage across the KB (Figure 10). Throughout the PS and lower Akchagylian, a combination of the C2An.3n and C2An.1n chrons allows for generally consistent correlations across the KFTB and KB. Correlation across the C2An.3n chron in Lokbatan, Jeirankechmez, and Babazanan indicates that during the mid to upper portions of the PS at ~3.5 Ma, a fluvio-deltaic environment persisted in the easternmost extent of the KB. The source for this deltaic system would likely be the paleo-Kura Delta for Babazanan, and most likely the paleo-Volga Delta for both Lokbatan and Jeirankechmez. The C2An.1n chron encompasses the upper PS – lower Akchagylian stage found at Jeirankechmez, Babazanan, Hajigabul (?), Kvabebi, and Kushkuna sections. This chron marks a consistent basin lithologic change from coarse – fine sandstones, to thickly bedded siltstones and claystones. This indicates that that Caspian Sea transgressed into the furthest western reaches of the KB during the Akchagylian, agreeing with regional geologic maps of Azerbaijan by Ali-Zade (2005). There is a distinct difference in the age of the Akchagylian stage boundary and depositional environments between the western sections and eastern sections. The Akchagylian transgression in the western extent of the Kura Basin reflects a relatively stable coastline that readily transitioned to a more terrestrial fluvial environment marked by an increase in the overall grain-size and the disappearance of both fresh and brackish water fauna (e.g., Jorissen, 2020). These differences, coupled with depositional environment interpretations could reflect freshwater inundation reaching the western KB almost instantly at 2.95 Ma, with freshwater conditions not being as favorable further east within the KB.

The Olduvai chron is present in lower to mid-Apsheronian deposits found in Lokbatan, Jeirankechmez, Hajigabul, Göychay, and Xocashen. During the Olduvai chron, the KB experienced lateral changes in depositional environments along strike.

At Lokbatan and Jeirankechmez at ~1.7 Ma a brackish, shallow to deepwater, lacustrine environment persisted. This deepwater lacustrine environment transitioned to a nearshore coastal environment with lagoonal development further west in Hajigabul. The coastal and lagoonal environment gives way further west to fluvio-deltaic and marginal lacustrine environments with coarse sediment derived from. the actively deforming KFTB. Based on lithologic interpretations, the coarse-grained environment persists further west in Sarica where fluvial and alluvial depositional environments are present. The Bozdagh and Xocashen sections reflect a distally sourced fluvial environment along the margins of lacustrine environment. The variability of depositional environments along strike of the KFTB during the Apsheronian reflect a typical progression from terrestrial/transitional environments in which longstanding fluvial systems are feeding sediment into water-filled basin undergoing regressive and transgressive fluctuations (Boyd et al., 1992).

4.3. Response Times of the Kura Basin

4.3.1. Response Times Across the Total Width of the Kura Basin

To better understand the preservation potential of environmental signals with different periodicities across the KB, response times were calculated at 10-km intervals along each of the 8 roughly GC-perpendicular swaths, with the weighted average A value determined by the ratio of fluvial environments along each. In addition to calculating the maximum response time within the different cross-sections, we also calculated estimated response times as a function of distance from the approximated rangefront of the GC. This allows us to generate contours of expected response times, which we then use to estimate response times within given measured sections during different depositional stages (Figures 6, 7 and 9). The maximum response time was calculated using each swath's maximum L value, or the Kura River's average position in the PS case, given a range of pre-determined rainfall rates based on the paleoclimatic interpretations (Figure 11, Table 1). Specifically, we consider the PS to be a dry period, the Akchagyl as a wet period, and the Apsheron as a complicated setting, though for the purposes of our estimation, as a dry period.

As these basin response time calculations are estimations at best, we will base interpretations on the "representative climate" and report the values for both the wetter and drier climatic conditions.

The maximum basin response times for the PS, between 4 - 3 Ma, were calculated with a "representative" rainfall rate of 0.3 m/yr and an A value of 0.15. Each swath yields a response time > 10^6 years, and except for swath 2 and 3, are within range of the initiation of rapid uplift in the GC between 5 – 10 Ma. The maximum response times of the swaths range from ~ 6 Ma to ~12 Ma, with a minimum value of 6 Ma occurring along swaths 5 & 7, and a maximum value of ~12 Ma along swath 2 (Figure 11). The response times in the westernmost parts of the KB (swaths 1 – 3) are greater than the easternmost KB (swaths 6 – 8) (Figure 11).

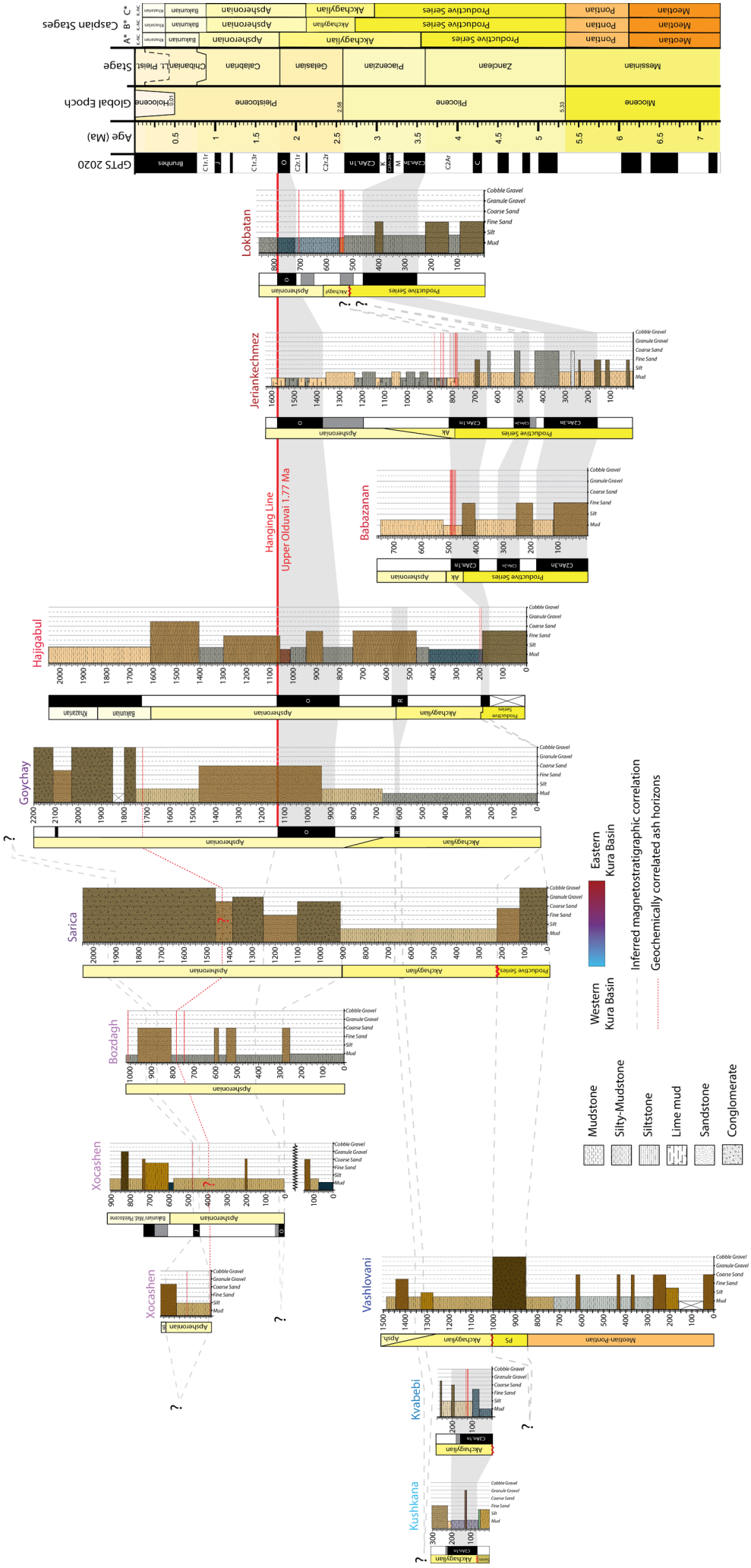

Figure 10 | Generalized measured stratigraphic section within the Kura Basin. Sections are roughly oriented from left to right in an east to west orientation. Warmer red colors = Eastern measured section. Darker blue-purple colors = Western measured sections. Bold red line = Olduvai chron hanging line. Lithologies in each section are colored based on field descriptions.

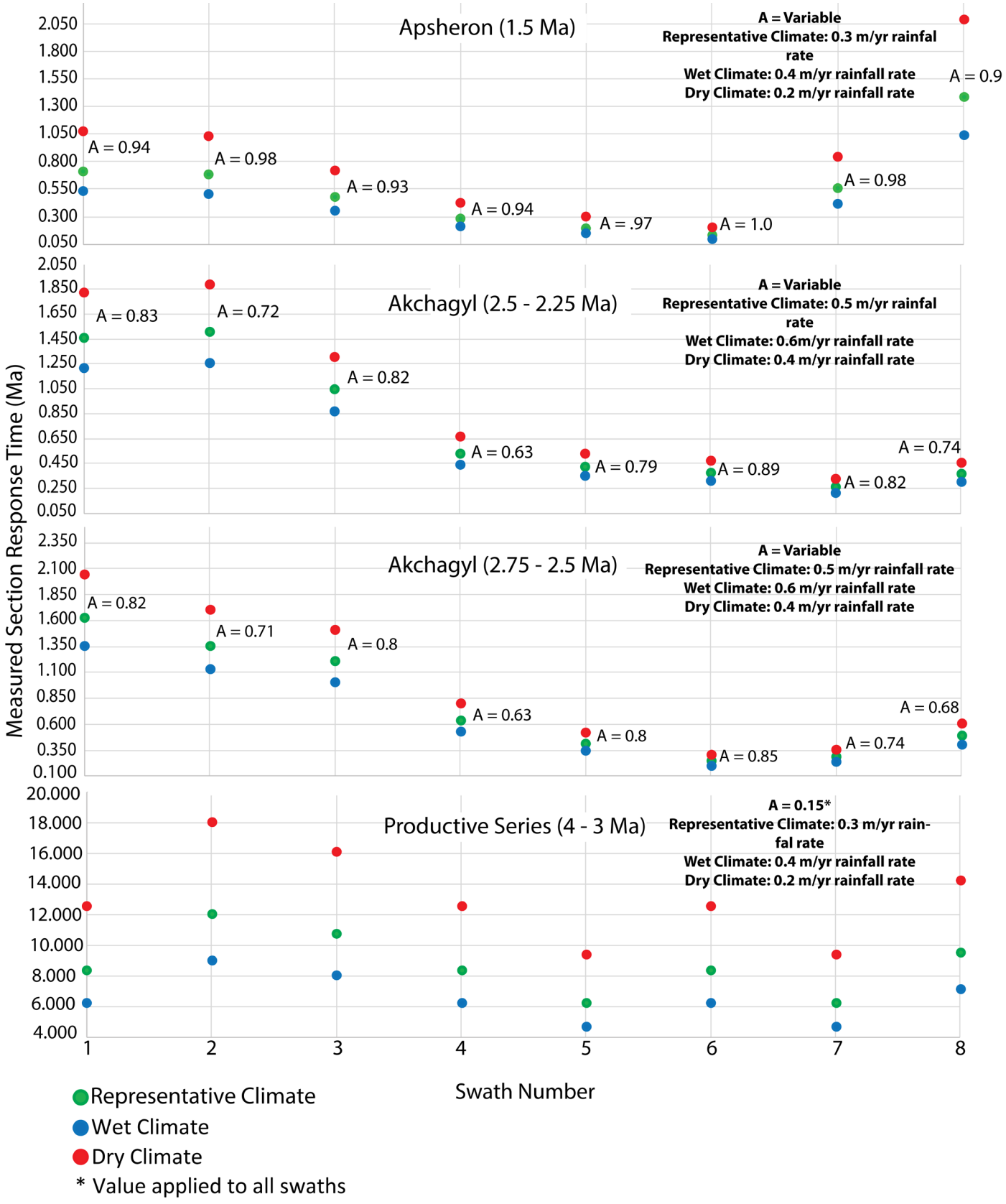

Figure 11 | Calculated maximum basin response times across the Kura Basin. Green dot = Calculated maximum response time for the representative climate, red circle = calculated response time for drier climate, blue circle = calculated response time for wet climate. Swath number are ordered from west (1) to east (8).

For the early Akchagyl between 2.75 to 2.5 Ma, given a "representative" rainfall rate of 0.5 m/yr, and variable A values (see Figure 11 for the calculated A value for each swath), the maximum basin response times range from ~1.6 Ma - ~0.3 Ma, with a minimum value of 0.3 Ma at swath 6 and a maximum value of 1.6 Ma occurring at swath 1. For the later Akchagyl from 2.5 to 2.25 Ma, we use the same "representative" rainfall rate, but updated variable A values based on the paleogeography (see Figure 11). The maximum basin response times for this later portion of the Akchagyl range from ~1.5 Ma - 0.25 Ma, with a minimum value of 0.25 Ma at swath 7 and a maximum value of 1.5

Measured Sections	Productive Series (4 - 3 Ma)			Akchagyl (2.75 - 2.5 Ma)			Akchagyl (2.5 - 2.25 Ma)			Apsheron (1.5 - 1.4 Ma)		
	Optimum Climate	*Wet Climate*	*Dry Climate*	*Optimum Climate*	*Wet Climate*	*Dry Climate*	*Optimum Climate*	*Wet Climate*	*Dry Climate*	*Optimum Climate*	*Wet Climate*	*Dry Climate*
Kushkuna	-	-	-	~1.6 Ma	~1.4 Ma	~2 Ma	~1.5 Ma	~1.2 Ma	~1.8 Ma	-	-	-
Kvabebi	-	-	-	~0.8 Ma	~0.7 Ma	~1 Ma	~0.8 Ma	~0.7 Ma	~1 Ma	-	-	-
Vashlovani	~10 Ma	~8 Ma	~16 Ma	~0.8 Ma	~0.9 Ma	~1 Ma	~0.8 Ma	~0.7 Ma	~1.1 Ma	~0.2 Ma	~0.16 Ma	~0.3 Ma
Xocashen	-	-	-	-	-	-	-	-	-	~0.2 Ma	~0.16 Ma	~0.3 Ma
Bozdagh	-	-	-	-	-	-	-	-	-	-	-	-
Sarica	~7 Ma	~5.5 Ma	~11 Ma	~0.5 Ma	~0.4 Ma	~0.7 Ma	~0.5 Ma	~0.4 Ma	~0.7 Ma	~.05 Ma	~0.04 Ma	~0.08 Ma
Göychay	-	-	-	-	-	-	-	-	-	~0.14 Ma	~0.10 Ma	~0.21 Ma
Hajigabul	~10 Ma	~7 Ma	~14 Ma	-	-	-	-	-	-	~0.9 Ma	~0.7 Ma	~1.5 Ma

Table 1 | Basin response times at each measured section throughout the Caspian Stages present at the published measured sections. Grey-dashed cells indicate no basin response time calculation due to the section not being active at the time, or because the section was not experiencing fluvial conditions.

Ma at swath 2. Both time slices from the Akchagylian yield similar results as seen in the PS, with the westernmost swath yielding greater response times than the eastern-most swaths, primarily reflecting the greater basin widths in the western KB during the Akchagyl.

The maximum basin response times for the Apsheron at ~1.5 Ma are calculated using a "representative" rainfall rate of 0.3 m/yr with variable A values for each swath. The maximum basin response times range from ~1.3 Ma to 0.09 Ma, with a minimum value of ~0.09 Ma occurring at swath 6 and a maximum value of 1.3 Ma at swath 8.

The Apsheron swaths follow a similar trend as seen in the PS and Akchagylian, with the westernmost swaths showing a slightly greater basin response time, with swaths 7 and 8 showing a reverse in this trend.

For our discussion of response times within individual measured sections, we focus on those for which we have relevant exposure of the time slice in question. For example, during the PS, while we can estimate the response time in many of the sections based on their reconstructed locations at that time, only the Vashlovani, Sarica, and Hajigabul sections actually have exposure of PS aged sediments, and thus we focus our discussion on those sections. Given the chosen representative climate conditions of the three sections, Vashlovani and Hajigabul have the greatest response time of 10 Ma, followed by Sarica with response times of 7 Ma (Table 1). During the Akchagyl from 2.75 – 2.5 Ma, the Kushkuna, Kvabebi, Vashlovani, and Sarica sections are active. Kushkuna has a greater response time of 1.6 Ma, followed by Vashlovani, Kvabebi, and Sarica with response times of 0.8 Ma, 0.8 Ma, and 0.5 Ma, respectively (Table 1). During the Akchagylian from 2.5 – 2.25 Ma, the Kushkuna, Kvabebi, Vashlovani, Sarica sections are active. The greatest response time occurs at Kushkuna with a value of 1.5 Ma, followed by Sarica, Kvabebi, Vashlovani with values of 0.8 Ma (for both Kvabebi and Vashlovani), and 0.5 Ma, respectively (Table 1). During the Apsheron at ~1.5 Ma, the Vashlovani, Xocashen, Sarica, Göychay, and Hajigabul sections are all active. Hajigabul has the greatest response time of 0.9 Ma, followed by Xocashen, Göychay, Vashlovani, and Sarica, with values of 0.2 Ma, 0.14 Ma, 0.2 Ma, and 0.05 Ma, respectively (Table 1).

4.3.2. Kura Basin Response Times and the Possibility of Preserving Tectonic and Climatic Signals

As stated in Section 1, basin response times can act as a first-order proxy for assessing what types of signals (tectonic or climatic) could be preserved within the stratigraphy, or the extent to which either signal could be reliably recorded. However, it is important to consider these basin response times with some degree of skepticism due to the variety of sources of inherent uncertainty, including rainfall estimates across the Caspian Sea stages due to a lack of paleo-rainfall reconstructions in the region – which can be considered to impart uncertainty both in terms of magnitude but also along-strike patterns, as we effectively assume no along-strike patterns in precipitation, uncertainties in the position of the measured sections throughout time due to the paleogeographic reconstructions being done relative to a stable Eurasia, uncertainties pertaining to the amount of shortening within the KFTB, the transitions between fluvial environment types are gradational (i.e., a single A value is problematic), and the original concepts for the basin response time are focused on strictly terrigenous basins and thus are not transportable to portions of the basin deposited during lacustrine or marine conditions.

Across the KB, given the maximum basin width along the swaths for the Productive Series between 4 -3 Ma, the response times for all swaths are on a $>10^6$ yr timescale (Figure 11). Due to this, these sections, and likely the KB, would in theory preferentially record tectonic signals within its stratigraphy, and climatic signals will likely be lost or overprinted by tectonic processes. This does not rule out the possibility of climatic signals within the KB, especially in Hajigabul, since the response time for this section is from the extrapolation of response time contours beyond the extent of the swaths. However, it's critical to consider that our estimations suggest response times during the PS that are comparable to the "age" of the GC, i.e., the timescale over which rapid exhumation of the range has occurred (e.g., Vincent et al., 2020; Forte et al., 2022a), and

thus our results imply that the extent to which PS sediments might record this rapid exhumation is questionable. In other words, the combination of a response time of ~10 Ma during the deposition of 4-3 Ma PS sediments and an estimated start of rapid exhumation within the core of the GC at 10-5 Ma, would imply that the PS sediments would have limited capacity to record this change.

It is key to point out that these basin response times are ultimately a lag time assessment and should not be conflated sediment transport time. This difference becomes readily apparent when taking into account the sediment provenance work done throughout the KB (e.g., Abdullayev et al., 2018; Forte et al., 2023), which points towards the GC flysch becoming a sediment source throughout the Plio-Pleistocene Caspian stages.

For the Akchagyl from 2.75 – 2.5 Ma, the maximum basin response times, and basin response times of individual sections Kushkuna, Kvabebi, Vashlovani, and Sarica are all on a time scale of 10^5 - 10^6 years (Figure 11, Table1). This indicates that the KB could record either long periodicity climatic cycles (especially in the eastern KB) (i.e., Milankovitch Cycles), or shorter tectonic cycles. It is a non-trivial task to determine which is more likely preserved. Given that the response times during this time slice show basin response time $>10^6$ years in the west and 10^5 years in the east, it is more likely that climatic processes are preserved in the eastern KB. The Akchagyl, from 2.5 – 2.25 Ma, and Apsheron at ~1.5 Ma, are unique compared to the PS and later Akchagyl reconstructions due to their relationship with activation of the KFTB. During the Akchagyl from 2.5 Ma – 2.25 Ma across the KB and KFTB, the basin response times exhibit the same trend as the Akchagyl from 2.75 – 2.25 Ma (Figure 11, Table 1). During the Apsheron, the maximum basin response times across the KB and KFTB are $<10^5$ years, with response times for the individual measured sections mostly $<10^5$ years (Figure 11, Table 1). At a first-order observation, and following previous interpretations stated above, this should indicate the preservation of climatic signals over tectonic signals, with individual measured sections within the Apsheron stage capturing lower periodicity cycles (e.g., eccentricity on 100 kya cycles and obliquity on 41 kya cycles). The basin response times in this study can act as a way to calculate the lower limits of the types of signals that could be preserved. Since the Akchagyl and Apsheron during these time slices yield response times $< 10^{4-6}$ years, and the prevalent tectonic activity occurring during this stage, either tectonic or climatic signals could be preserved.

5. Conclusions

In this synthesis, we present a suite of paleogeographic reconstructions coupled with depositional environment interpretations from prior work on KFTB measured sections, to give a more accurate and holistic view of the stratigraphic context of the Pliocene –Pleistocene development of the KB and KFTB. This synthesis is a reference for the significant tectono-climatic events occurring in and around the GC, their timing relative to the Caspian Stages, and the most up-to-date age models of the Caspian Stages. We use our paleogeographic and paleoenvironmental synthesis to determine if the changes in the tectonic and climatic boundary conditions adjacent to the foreland basin of a young orogen are likely to be preserved within the foreland stratigraphy.

5.1. Correlation of the Depositional Environments Across the Plio-Pleistocene Kura Basin

The KB and KFTB stratigraphy differ significantly along the strike of the basin, but also within the same Caspian Stage at different points within the basin. This study showcases that the direct lithologic correlation between different Caspian Stages within the Caucasus is complex. Instead, focusing on mixtures of chrono-, magneto-, and biostratigraphic methods for correlation of the KFTB Plio-Pleistocene strata are essential. Our new correlations and synthesis of available magnetostratigraphic and environmental indicators allow us to make several key observations regarding the depositional environments that persisted at key Caspian Stages.

1) During the Productive Series, between 4 – 3 Ma, long-standing fluvial-deltaic environments persisted throughout the easternmost KB adjacent to the SCB. These deltaic systems belonged to the paleo-Kura and paleo-Volga rivers, emptying into the SCB. The C2An.3n chron correlates between Lokbatan, Jeirankechmez, and Babazanan, which all describe the PS as fluvial-deltaic environments with well-developed floodplains. The upper portion of the PS can be correlated between Jeirankechmez, Babazanan, and Hajigabul in the eastern KB, and at Kvabebi and Kushkuna in the far western KB using the C2An.1n chron. This chron is of crucial importance within the Caucasus as it encompasses the upper PS/Akchagyl stage boundary and a marked lithologic switch from coarse-grained sandstones to siltstones and mudstones. This lithologic switch is substantial because it occurs nearly instantaneously across the KB and is refined by palynological analyses and radiometric dating of ash beds within the lower Akchagyl. This transition to Akchagyl is marked by the freshwater inundation to the western extent of the Kura Basin.

2) The Apsheron across the KFTB can be correlated reliably with Olduvai chron. During the Olduvai chron, the KFTB was experiencing variable depositional environments along strike. Lokbatan, Jeirankechmez, Hajigabul, and Babazanan experience marginal lacustrine to coastal and distal brackish water depositional environments. While moving further west into the central eastern to western portions of the KFTB, into the Göychay, Sarica, Xocashen, Bozdagh, and Vashlovani localities, meandering fluvial environments transition to deltaic environments, which then transition to coastal environments within the KB. This follows a general coarsening upward trend found

throughout most of the Apsheronian deposits moving westward.

5.2. Key Points from Basin Response Time Assessment

Using basin response time calculations as a first-order proxy for interpreting the possible roles of tectonics and climate on KB stratigraphy within the Caucasus offers a unique opportunity to understand how foreland stratigraphy reflects the changes in these boundary conditions. Focusing on maximum response times, from estimates of regional precipitation rates and paleogeography during the Productive Series, response times > 10^6 years suggest that tectonic signals would likely be preserved within this portion of the KB stratigraphy. Although the response time calculations indicate a preference for tectonic signals, climatic signals cannot be ruled out, especially within the eastern portion of the KB, due to the proximity to the Caspian Sea. In contrast, response times estimated for the early Akchagyl reconstruction all yield values <10^5 years, indicating that long periodicity climatic cycles (i.e., Milankovitch Cycles) or shorter periodicity tectonic processes could be preserved. Generally, major tectonic changes are not readily apparent in early Akchagyl stratigraphy throughout much of the KB, making the preservation of climatic signals more likely. Contrastingly, the latter Akchagyl and Apsheron reconstructions yield maximum basin response times and measure section response times <10^4 – 10^5 years. This would initially indicate that KB and measured sections could preferentially record shorter periodicity climatic signals. However, this is complicated by the activation of the KFTB within these two reconstruction time slices. The migration of the deformation front of the GC south into the KB results in both a shortening of the basin width, influencing the basin response time, and the fact that active tectonics are feeding sediment directly into these measured sections, often resulting in a coarse-grained sediment caliber. This possible tectonic influence and the conflicting basin response time results could indicate that neither signal will be discernable using basin response time, or that some combination of the two processes is influencing stratigraphy, with neither forcing dominant.

The basin response time calculations show that foreland basins likely record different types of signals at various times throughout their development. This also highlights the necessity of detailed description, correlation, dating, structural, and climatic investigations of foreland stratigraphy, and the utility of placing that stratigraphy into paleogeographic contexts to understand the possible significance of apparent environmental signals preserved in foreland strata.

Acknowledgements

We thank reviewers Dr. Syu-Heng Lai and Dr. Sergei Lazarev who both aided with incredibly helpful and insightful comments on an earlier draft of this manuscript. We thank Associate Editor Dr. Julien Bailleul for assistance for their guidance in the review and submission processes. We also thank Dr. Ryan Leary for insightful conversations regarding basin response times.

Authors contribution

Primary Study Design, Writing, Calculations, and Figure Development: Kristoffer Fowler. Secondary Study Design and Writing: Adam Forte.

Data availability

The authors confirm that the data supporting the findings of this study are available within the article.

Conflict of interest

The authors declare that they have no known competing financial interests or personal relationships that could have influenced the work reported in this paper.

References

Abdullayev, N. R., Weber, J., Baak, C. G. C. van, Aliyeva, E., Leslie, C., Riley, G. W., O'Sullivan, P., & Kislitsiyn, R. (2018). Detrital zircon and apatite constraints on depositional ages, sedimentation rates and provenance: Pliocene Productive Series, South Caspian Basin, Azerbaijan. Basin Research, 30(5), 835–862. https://doi.org/10.1111/bre.12283

Adamia, S., Alania, V., Chabukiani, A., Kutelia, Z., & Sadradze, N. (2011a). Great Caucasus (Cavcasioni): A Long-lived North-Tethyan Back-Arc Basin. Turkish Journal of Earth Sciences, 20(5), 611–628. https://doi.org/10.3906/yer-1005-12

Adamia, S., Zakariadze, G., Chkhotua, T., Sadradze, N., Tsereteli, N., Chabukiani, A., & Gventsadze, A. (2011b). Geology of the Caucasus: A Review. Turkish Journal of Earth Sciences. https://doi.org/10.3906/yer-1005-11

Adamia, Sh. A., Lordkipanidze, M. B., & Zakariadze, G. S. (1977). Evolution of an active continental margin as exemplified by the Alpine history of the Caucasus. Tectonophysics, 40(3), 183–199. https://doi.org/10.1016/0040-1951(77)90065-8

Agustí, J., Vekua, A., Oms, O., Lordkipanidze, D., Bukhsianidze, M., Kiladze, G., & Rook, L. (2009). The Pliocene-Pleistocene succession of Kvabebi (Georgia) and the background to the early human occupation of Southern Caucasus. Quaternary Science Reviews, 28(27–28), 3275–3280. https://doi.org/10.1016/j.quascirev.2009.09.001

Aghayeva, V., Sachsenhofer, R. F., van Baak, C. G. C., Bayramova, Sh., Ćorić, S., Frühwirth, M. J., Rzayeva, E., & Vincent, S. J. (2023). Stratigraphy of the Cenozoic succession in eastern Azerbaijan: Implications for petroleum systems and paleogeography in the Caspian basin. Marine and Petroleum Geology, 150, 106148. https://doi.org/10.1016/j.marpetgeo.2023.106148

Alania, V., Enukidze, O., Glonti, N., Razmadze, A., Chabukiani, A., Giorgadze, A., Glonti, B. V., Koiava, K., Beridze, T., Khutsishvili, S., & Chagelishvili, R. (2018). Structural Architecture of the Kura Foreland Fold-and-thrust Belt Using Seismic Reflection Profile, Georgia. Universal Journal of Geoscience, 6(6), 184–190. https://doi.org/10.13189/ujg.2018.060602

Alania, V. M., Chabukiani, A. O., Chagelishvili, R. L., Enukidze, O. V., Gogrichiani, K. O., Razmadze, A. N., & Tsereteli, N. S.

(2017). Growth structures, piggy-back basins and growth strata of the Georgian part of the Kura foreland fold–thrust belt: Implications for Late Alpine kinematic evolution. Geological Society, London, Special Publications, 428(1), 171–185. https://doi.org/10.1144/SP428.5

Ali-Zade, A. A. (2005). Geological Map of Azerbaijan Republic. Scale 1: 500,000 [Geologic Map]. National Academy of Sciences of Azerbaijan Republic Geology Institute, Baku, Azerbaijan.

Ali-Zade, A. A., Alizade, K. A., Aleskerov, D. A., Buleishvili, D. A., Vekua, A. K., Konstantinova, N. A., Lebedeva, K. N. N.-N., Bikiforova, K. V., Pevzner, M. A., Khubka, A. N., Chepalyga, A. I., & Chernyakhovsky, A. G. (1972). Guidebook: Excursions in Moldavia, Georgia, Azerbaijan. (Vol. 105). IUGS Subcommission on Neogene Stratigraphy.

Allen, J. P., Fielding, C. R., Rygel, M. C., & Gibling, M. R. (2013). Deconvolving Signals of Tectonic and Climatic Controls From Continental Basins: An Example From the Late Paleozoic Cumberland Basin, Atlantic Canada. Journal of Sedimentary Research, 83(10), 847–872. https://doi.org/10.2110/jsr.2013.58

Allen, M. B., & Armstrong, H. A. (2008). Arabia–Eurasia collision and the forcing of mid-Cenozoic global cooling. Palaeogeography, Palaeoclimatology, Palaeoecology, 265(1), 52–58. https://doi.org/10.1016/j.palaeo.2008.04.021

Allen, M., Jackson, J., & Walker, R. (2004). Late Cenozoic reorganization of the Arabia-Eurasia collision and the comparison of short-term and long-term deformation rates. Tectonics, 23(2), https://doi.org/10.1029/2003TC001530

Allen, M., Jones, S., Ismail-Zadeh, A., Simmons, M., & Anderson, L. (2002). Onset of subduction as the cause of rapid Pliocene-Quaternary subsidence in the South Caspian basin. Geology, 30(9), 775–778. https://doi.org/10.1130/0091-7613(2002)030%3C0775:OOSATC%3E2.0.CO;2

Armitage, J. J., Duller, R. A., Whittaker, A. C., & Allen, P. A. (2011). Transformation of tectonic and climatic signals from source to sedimentary archive. Nature Geoscience, 4(4), 231–235. https://doi.org/10.1038/ngeo1087

Avdeev, B., & Niemi, N. A. (2011). Rapid Pliocene exhumation of the central Greater Caucasus constrained by low-temperature thermochronometry: RAPID EXHUMATION OF THE GREATER CAUCASUS. Tectonics, 30(2), https://doi.org/10.1029/2010TC002808

Axen, G. J., Lam, P. S., Grove, M., Stockli, D. F., & Hassanzadeh, J. (2001). Exhumation of the west-central Alborz Mountains, Iran, Caspian subsidence, and collision-related tectonics. Geology, 29(6), 559–562. https://doi.org/10.1130/0091-7613(2001)029<0559:EOTWCA>2.0.CO;2

Ballato, P., Uba, C. E., Landgraf, A., Strecker, M. R., Sudo, M., Stockli, D. F., Friedrich, A., & Tabatabaei, S. H. (2011). Arabia-Eurasia continental collision: Insights from late Tertiary foreland-basin evolution in the Alborz Mountains, northern Iran. Geological Society of America Bulletin, 123(1–2), 106–131. https://doi.org/10.1130/B30091.1

Barber, D. E., Stockli, D. F., Horton, B. K., & Koshnaw, R. I. (2018). Cenozoic Exhumation and Foreland Basin Evolution of the Zagros Orogen During the Arabia-Eurasia Collision, Western Iran. Tectonics, 37(12), 4396–4420. https://doi.org/10.1029/2018TC005328

Bartoli, G., Sarnthein, M., Weinelt, M., Erlenkeuser, H., Garbe-Schönberg, D., & Lea, D. W. (2005). Final closure of Panama and the onset of northern hemisphere glaciation. Earth and Planetary Science Letters, 237(1), 33–44. https://doi.org/10.1016/j.epsl.2005.06.020

Böhme, M., Spassov, N., Majidifard, M. R., Gärtner, A., Kirscher, U., Marks, M., Dietzel, C., Uhlig, G., El Atfy, H., Begun, D. R., & Winklhofer, M. (2021). Neogene hyperaridity in Arabia drove the directions of mammalian dispersal between Africa and Eurasia. Communications Earth & Environment, 2(1), 85. https://doi.org/10.1038/s43247-021-00158-y

Borisov, A. A., & Halstead, C. A. (1965). Climates of the U.S.S.R (Location Information LSU Library (Main Collection)) [Book]. Aldine Pub. Co.

Boyd, R., Dalrymple, R., & Zaitlin, B. A. (1992). Classification of clastic coastal depositional environments. Sedimentary Geology, 80(3), 139–150. https://doi.org/10.1016/0037-0738(92)90037-R

Brocklehurst, S. H., & Whipple, K. X. (2004). Hypsometry of glaciated landscapes. Earth Surface Processes and Landforms, 29(7), 907–926. https://doi.org/10.1002/esp.1083

Caracciolo, L. (2020). Sediment generation and sediment routing systems from a quantitative provenance analysis perspective: Review, application and future development. Earth-Science Reviews, 209, 103226. https://doi.org/10.1016/j.earscirev.2020.103226

Caracciolo, L., Ravidà, D. C. G., Chew, D., Janßen, M., Lünsdorf, N. K., Heins, W. A., Stephan, T., & Stollhofen, H. (2021). Reconstructing environmental signals across the Permian-Triassic boundary in the SE Germanic Basin: A Quantitative Provenance Analysis (QPA) approach. Global and Planetary Change, 206, 103631. https://doi.org/10.1016/j.gloplacha.2021.103631

Castelltort, S., & Van Den Driessche, J. (2003). How plausible are high-frequency sediment supply-driven cycles in the stratigraphic record? Sedimentary Geology, 157(1), 3–13. https://doi.org/10.1016/S0037-0738(03)00066-6

Connor, S. E., & Kvavadze, E. V. (2009). Modelling late Quaternary changes in plant distribution, vegetation and climate using pollen data from Georgia, Caucasus. Journal of Biogeography, 36(3), 529–545. https://doi.org/10.1111/j.1365-2699.2008.02019.x

Cowgill, E., Forte, A. M., Niemi, N., Avdeev, B., Tye, A., Trexler, C., Javakhishvili, Z., Elashvili, M., & Godoladze, T. (2016). Relict basin closure and crustal shortening budgets during continental collision: An example from Caucasus sediment provenance: Greater Caucasus Relict Basin Closure. Tectonics, 35(12), 2918–2947. https://doi.org/10.1002/2016TC004295

Cromartie, A., Blanchet, C., Barhoumi, C., Messager, E., Peyron, O., Ollivier, V., Sabatier, P., Etienne, D., Karakhanyan, A., Khatchadourian, L., Smith, A. T., Badalyan, R., Perello, B., Lindsay, I., & Joannin, S. (2020). The vegetation, climate, and fire history of a mountain steppe: A Holocene reconstruction from the South Caucasus, Shenkani, Armenia. Quaternary Science Reviews, 246, 106485. https://doi.org/10.1016/j.quascirev.2020.106485

Darin, M. H., & Umhoefer, P. J. (2022). Diachronous initiation of Arabia–Eurasia collision from eastern Anatolia to the southeastern Zagros Mountains since middle Eocene time. International Geology Review, 64(18), 2653–2681. https://doi.org/10.1080/00206814.2022.2048272

de la Vara, A., van Baak, C. G. C., Marzocchi, A., Grothe, A., & Meijer, P. Th. (2016). Quantitative analysis of Paratethys sea level change during the Messinian Salinity Crisis. Marine Geology, 379, 39–51. https://doi.org/10.1016/j.margeo.2016.05.002

DeCelles, P. G., & Giles, K. A. (1996). Foreland basin systems. Basin Research, 8(2), 105–123. https://doi.org/10.1046/j.1365-2117.1996.01491.x

Egan, S. S., Mosar, J., Brunet, M.-F., & Kangarli, T. (2009). Subsidence and uplift mechanisms within the South Caspian Basin: Insights from the onshore and offshore Azerbaijan region. Geological Society, London, Special Publications, 312(1), 219–240. https://doi.org/10.1144/SP312.11

Ershov, A. V., Brunet, M.-F., Nikishin, A. M., Bolotov, S. N., Nazarevich, B. P., & Korotaev, M. V. (2003). Northern Caucasus basin: Thermal history and synthesis of subsidence models. Sedimentary Geology, 156(1), 95–118. https://doi.org/10.1016/S0037-0738(02)00284-1

Forte, A. M., Cowgill, E., Bernardin, T., Kreylos, O., & Hamann, B. (2010). Late Cenozoic deformation of the Kura fold-thrust belt, southern Greater Caucasus. Geological Society of America Bulletin, 122(3–4), 465–486. https://doi.org/10.1130/B26464.1

Forte Adam M. (2012). Late Cenozoic Evolution of the Greater Caucasus Mountains and Kura Foreland Basin: Implications for Early Orogenesis - ProQuest. https://www.proquest.com/openview/3db604862ab5a0ffa76603bb287ce0c9/1?pq-origsite=gscholar&cbl=18750

Forte, A. M., & Cowgill, E. (2013a). Late Cenozoic base-level variations of the Caspian Sea: A review of its history and proposed driving mechanisms. Palaeogeography, Palaeoclimatology, Palaeoecology, 386, 392–407. https://doi.org/10.1016/j.palaeo.2013.05.035

Forte, A. M., Cowgill, E., Murtuzayev, I., Kangarli, T., & Stoica, M. (2013b). Structural geometries and magnitude of shortening in the eastern Kura fold-thrust belt, Azerbaijan: Implications for the development of the Greater Caucasus Mountains. Tectonics, 32(3), 688–717. https://doi.org/10.1002/tect.20032

Forte, A. M., Cowgill, E., & Whipple, K. X. (2014). Transition from a singly vergent to doubly vergent wedge in a young orogen: The Greater Caucasus: Greater Caucasus tectonic zonation. Tectonics, 33(11), 2077–2101. https://doi.org/10.1002/2014TC003651

Forte, A. M., Sumner, D. Y., Cowgill, E., Stoica, M., Murtuzayev, I., Kangarli, T., Elashvili, M., Godoladze, T., & Javakhishvili, Z. (2015a). Late Miocene to Pliocene stratigraphy of the Kura Basin, a subbasin of the South Caspian Basin: Implications for the diachroneity of stage boundaries. Basin Research, 27(3), 247–271. https://doi.org/10.1111/bre.12069

Forte, A. M., Whipple, K. X., & Cowgill, E. (2015b). Drainage network reveals patterns and history of active deformation in the eastern Greater Caucasus. Geosphere, 11(5), 1343–1364. https://doi.org/10.1130/GES01121.1

Forte, A. M., Whipple, K. X., Bookhagen, B., & Rossi, M. W. (2016). Decoupling of modern shortening rates, climate, and topography in the Caucasus. Earth and Planetary Science Letters, 449, 282–294. https://doi.org/10.1016/j.epsl.2016.06.013

Forte, A. M., Gutterman, K. R., Soest, M. C., & Gallagher, K. (2022a). Building a Young Mountain Range: Insight Into the Growth of the Greater Caucasus Mountains From Detrital Zircon (U-Th)/He Thermochronology and 10Be Erosion Rates. Tectonics, 41(5). https://doi.org/10.1029/2021TC006900

Forte, A. M., Leonard, J. S., Rossi, M. W., Whipple, K. X., Heimsath, A. M., Sukhishvili, L., Godoladze, T., & Kadirov, F. (2022b). Low variability runoff inhibits coupling of climate, tectonics, and topography in the Greater Caucasus. Earth and Planetary Science Letters, 584, 117525. https://doi.org/10.1016/j.epsl.2022.117525

Forte, A. M., Cowgill, E., Sumner, D., Garello, D., Niemi, N., & Fowler, K. (2023). Timing and Evolution of Structures within the Southeastern Greater Caucasus and Kura Fold-Thrust Belt from Multiproxy Sediment Provenance Records [Preprint]. Earth Sciences. https://doi.org/10.31223/X5996K

Gobejishvili, R., Lomidze, N., & Tielidze, L. (2011). Chapter 12—Late Pleistocene (Würmian) Glaciations of the Caucasus. In J. Ehlers, P. L. Gibbard, & P. D. Hughes (Eds.), Developments in Quaternary Sciences (Vol. 15, pp. 141–147). Elsevier. https://doi.org/10.1016/B978-0-444-53447-7.00012-X

Green, T., Abdullayev, N., Hossack, J., Riley, G., & Roberts, A. M. (2009). Sedimentation and subsidence in the South Caspian Basin, Azerbaijan. Geological Society, London, Special Publications, 312(1), 241–260. https://doi.org/10.1144/SP312.12

Gunnels, M., Yetrimishli, G., Kazimova, S., & Sandvol, E. (2020). Seismotectonic evidence for subduction beneath the Eastern Greater Caucasus. Geophysical Journal International, 224(3), 1825–1834. https://doi.org/10.1093/gji/ggaa522

Heller, P. L., & Paola, C. (1992). The large-scale dynamics of grain-size variation in alluvial basins, 2: Application to syntectonic conglomerate. Basin Research, 4(2), 91–102. https://doi.org/10.1111/j.1365-2117.1992.tb00146.x

Hinds, D. J., Aliyeva, E., Allen, M. B., Davies, C. E., Kroonenberg, S. B., Simmons, M. D., & Vincent, S. J. (2004). Sedimentation in a discharge dominated fluvial-lacustrine system: The Neogene Productive Series of the South Caspian Basin, Azerbaijan. Marine and Petroleum Geology, 21(5), 613–638. https://doi.org/10.1016/j.marpetgeo.2004.01.009

Hoyle, T. M., Leroy, S. A. G., López-Merino, L., & Richards, K. (2018). Using fluorescence microscopy to discern in situ from reworked palynomorphs in dynamic depositional environments—An example from sediments of the late Miocene to early Pleistocene Caspian Sea. Review of Palaeobotany and Palynology, 256, 32–49. https://doi.org/10.1016/j.revpalbo.2018.05.005

Hoyle, T. M., Leroy, S. A. G., López-Merino, L., van Baak, C. G. C., Martínez Cortizas, A., Richards, K., & Aghayeva, V. (2021). Biological turnovers in response to marine incursion into the Caspian Sea at the Plio-Pleistocene transition. Global and Planetary Change, 206, 103623. https://doi.org/10.1016/j.gloplacha.2021.103623

Hoyle, T. M., Leroy, S. A. G., López-Merino, L., Miggins, D. P., & Koppers, A. A. P. (2020). Vegetation succession and climate change across the Plio-Pleistocene transition in eastern Azerbaijan, central Eurasia (2.77–2.45 Ma). Palaeogeography, Palaeoclimatology, Palaeoecology, 538, 109386. https://doi.org/10.1016/j.palaeo.2019.109386

Hsü, K. J., Montadert, L., Bernoulli, D., Cita, M. B., Erickson, A., Garrison, R. E., Kidd, R. B., Mèlierés, F., Müller, C., & Wright, R. (1977). History of the Mediterranean salinity crisis. Nature, 267(5610), 399–403. https://doi.org/10.1038/267399a0

Jackson, J., Priestley, K., Allen, M., & Berberian, M. (2002). Active tectonics of the South Caspian Basin. Geophysical Journal International, 148(2), 214–245. https://doi.org/10.1046/j.1365-246X.2002.01588.x

Jones, R. W., & Simmons, M. D. (1997). A review of the stratigraphy of eastern Paratethys (Oligocene-Holocene), with particular emphasis on the Black Sea. AAPG Memoir, 68, 39–51.

Jorissen, E. (2020). The Pontocaspian basins in a grain of sand: Coastal sedimentary architecture, forcing mechanisms, and faunal turnover events in restricted basins. Utrecht Studies in Earth Sciences, 209. https://dspace.library.uu.nl/handle/1874/396683

Jorissen, E. L., Abels, H. A., Wesselingh, F. P., Lazarev, S., Aghayeva, V., & Krijgsman, W. (2020). Amplitude, frequency and drivers of Caspian Sea lake-level variations during the Early Pleistocene and their impact on a protected wave-dominated coastline. Sedimentology, 67(1), 649–676. https://doi.org/10.1111/sed.12658

Kadirov, F., Floyd, M., Alizadeh, A., Guliev, I., Reilinger, R., Kuleli, S., King, R., & Nafi Toksoz, M. (2012). Kinematics of the eastern Caucasus near Baku, Azerbaijan. Natural Hazards, 63(2), 997–1006. https://doi.org/10.1007/s11069-012-0199-0

Koçyiğit, A., Yilmaz, A., Adamia, S., & Kuloshvili, S. (2001). Neotectonics of East Anatolian Plateau (Turkey) and Lesser Caucasus: Implication for transition from thrusting to strike-slip faulting. Geodinamica Acta, 14(1–3), 177–195. https://doi.org/10.1080/09853111.2001.11432443

Krijgsman, W., Hilgen, F. J., Raffi, I., Sierro, F. J., & Wilson, D. S. (1999). Chronology, causes and progression of the Messinian salinity crisis. Nature, 400(6745), 652–655. https://doi.org/10.1038/23231

Krijgsman, W., Tesakov, A., Yanina, T., Lazarev, S., Danukalova, G., Van Baak, C. G. C., Agustí, J., Alçiçek, M. C., Aliyeva, E., Bista, D., Bruch, A., Büyükmeriç, Y., Bukhsianidze, M., Flecker, R., Frolov, P., Hoyle, T. M., Jorissen, E. L., Kirscher, U., Koriche, S. A., Kroonenberg, S. B., Lordkipanidze, D., Oms, O., Rausch, L., Singarayer, J., Stoica, M., van de Velde, S., Titov, V. V., & Wesselingh, F. P. (2019). Quaternary time scales for the Pontocaspian domain: Interbasinal connectivity and faunal evolution. Earth-Science Reviews, 188, 1-40. https://doi.org/10.1016/j.earscirev.2018.10.013

Kroonenberg, S. B., Alekseevski, N. I., Aliyeva, E., Allen, M. B., Aybulatov, D. N., Baba-Zadeh, A., Badyukova, E. N., Davies, C. E., Hinds, D. J., Hoogendoorn, R. M., Huseynov, D., Ibrahimov, B., Mamedov, P., Overeem, I., Rusakov, G. V., Suleymanova, S., Svitoch, A. A., & Vincent, S. J. (2005). Two Deltas, Two Basins, One River, One Sea: The Modern Volga Delta as an Analogue of the Neogene Productive Series, South Caspian Basin. https://doi.org/10.2110/pec.05.83.0231

Lazarev, S., Jorissen, E. L., van de Velde, S., Rausch, L., Stoica, M., Wesselingh, F. P., Van Baak, C. G. C., Yanina, T. A., Aliyeva, E., & Krijgsman, W. (2019). Magneto-biostratigraphic age constraints on the palaeoenvironmental evolution of the South Caspian basin during the Early-Middle Pleistocene (Kura basin, Azerbaijan). Quaternary Science Reviews, 222, 105895. https://doi.org/10.1016/j.quascirev.2019.105895

Lazarev, S., Kuiper, K. F., Oms, O., Bukhsianidze, M., Vasilyan, D., Jorissen, E. L., Bouwmeester, M. J., Aghayeva, V., van Amerongen, A. J., Agustí, J., Lordkipanidze, D., & Krijgsman, W. (2021). Five-fold expansion of the Caspian Sea in the late Pliocene: New and revised magnetostratigraphic and 40Ar/39Ar age constraints on the Akchagylian Stage. Global and Planetary Change, 206, 103624. https://doi.org/10.1016/j.gloplacha.2021.103624

Lisiecki, L. E., & Raymo, M. E. (2005). A Pliocene-Pleistocene stack of 57 globally distributed benthic $\delta^{18}O$ records. Paleoceanography, 20(1). https://doi.org10.1029/2004pa001071

Lydolph, P. E. (1977). Climates of the Soviet Union. Elsevier Scientific Pub. Co.

McKenzie, D., Jackson, J., & Priestley, K. (2019). Continental collisions and the origin of subcrustal continental earthquakes. Canadian Journal of Earth Sciences, 56(11), 1101–1118. https://doi.org/10.1139/cjes-2018-0289

Milanovsky, E. E. (2008). Origin and development of ideas on Pliocene and Quaternary glaciations in northern and eastern Europe, Iceland, Caucasus and Siberia. Geological Society, London, Special Publications, 301(1), 87–115. https://doi.org/10.1144/SP301.6

Morton, A., Allen, M., Simmons, M., Spathopoulos, F., Still, J., Hinds, D., Ismail-Zadeh, A., & Kroonenberg, S. (2003). Provenance patterns in a neotectonic basin: Pliocene and Quaternary sediment supply to the South Caspian. Basin Research, 15(3), 321–337. https://doi.org/10.1046/j.1365-2117.2003.00208.x

Mosar, J., Kangarli, T., Bochud, M., Glasmacher, U. A., Rast, A., Brunet, M.-F., & Sosson, M. (2010). Cenozoic-Recent tectonics and uplift in the Greater Caucasus: A perspective from Azerbaijan. Geological Society, London, Special Publications, 340(1), 261–280. https://doi.org/10.1144/SP340.12

Müller, R. D., Cannon, J., Qin, X., Watson, R. J., Gurnis, M., Williams, S., Pfaffelmoser, T., Seton, M., Russell, S. H. J., & Zahirovic, S. (2018). GPlates: Building a Virtual Earth Through Deep Time. Geochemistry, Geophysics, Geosystems, 19(7), 2243–2261. https://doi.org/10.1029/2018GC007584

Nemčok, M., Glonti, B., Yukler, A., & Marton, B. (2013). Development history of the foreland plate trapped between two converging orogens; Kura Valley, Georgia, case study. Geological Society, London, Special Publications, 377(1), 159–188. https://doi.org/10.1144/SP377.9

Paola, C., Heller, P. L., & Angevine, C. L. (1992). The large-scale dynamics of grain-size variation in alluvial basins, 1: Theory. Basin Research, 4(2), 73–90. https://doi.org/10.1111/j.1365-2117.1992.tb00145.x

Philip, H., Cisternas, A., Gvishiani, A., & Gorshkov, A. (1989). The Caucasus: An actual example of the initial stages of continental collision. Tectonophysics, 161(1), 1–21. https://doi.org/10.1016/0040-1951(89)90297-7

Popov, S. V., Shcherba, I. G., Ilyina, L. B., Nevesskaya, L. A., Paramonova, N. P., Khondkarian, S. O., & Magyar, I. (2006). Late Miocene to Pliocene palaeogeography of the Paratethys and its relation to the Mediterranean. Palaeogeography, Palaeoclimatology, Palaeoecology, 238(1), 91–106. https://doi.org/10.1016/j.palaeo.2006.03.020

Raffi, I., Wade, B. S., Pälike, H., Beu, A. G., Cooper, R., Crundwell, M. P., Krijgsman, W., Moore, T., Raine, I., Sardella, R., & Vernyhorova, Y. V. (2020). Chapter 29—The Neogene Period. In F. M. Gradstein, J. G. Ogg, M. D. Schmitz, & G. M. Ogg (Eds.), Geologic Time Scale 2020 (pp. 1141–1215). Elsevier. https://doi.org/10.1016/B978-0-12-824360-2.00029-2

Ravidà, D. C. G., Caracciolo, L., Heins, W. A., & Stollhofen, H. (2021). Reconstructing environmental signals across the Permian-Triassic boundary in the SE Germanic basin: Paleodrainage modelling and quantification of sediment flux. Global and Planetary Change, 206, 103632. https://doi.org/10.1016/j.gloplacha.2021.103632

Reynolds, A. D., Simmons, M. D., Bowman, M. B. J., Henton, J., Brayshaw, A. C., Ali-Zade, A. A., Guliyev, I. S., Suleymanova, S. F., Ateava, E. Z., Mamedova, D. N., & Koshkarly, O. (1998). Implications of Outcrop Geology for Reservoirs in the Neogene Productive Series: Apsheron Peninsula, Azerbaijan. AAPG Bulletin, 82(1), 25–49. https://doi.org/10.1306/1D9BC38B-172D-11D7-8645000102C1865D

Richards, K., van Baak, C. G. C., Athersuch, J., Hoyle, T. M., Stoica, M., Austin, W. E. N., Cage, A. G., Wonders, A. A. H., Marret, F., & Pinnington, C. A. (2018). Palynology and micropalaeontology of the Pliocene - Pleistocene transition in outcrop from the western Caspian Sea, Azerbaijan: Potential links with the Mediterranean, Black Sea and the Arctic Ocean? Palaeogeography, Palaeoclimatology, Palaeoecology, 511, 119–143. https://doi.org/10.1016/j.palaeo.2018.07.018

Richards, K., Vincent, S. J., Davies, C. E., Hinds, D. J., & Aliyeva, E. (2021). Palynology and sedimentology of the Pliocene Productive Series from eastern Azerbaijan. Palynology, 45(4), 569–598. https://doi.org/10.1080/01916122.2021.1884139

Rögl, F. (1999). Mediterranean and Paratethys; facts and hypotheses of an Oligocene to Miocene paleogeography (short overview). Geologica Carpathica: International Geological Journal, 50(4), 339–349.

Romans, B. W., Castelltort, S., Covault, J. A., Fildani, A., & Walsh, J. P. (2016). Environmental signal propagation in sedimentary systems across timescales. Earth-Science Reviews, 153, 7–29. https://doi.org/10.1016/j.earscirev.2015.07.012

Stevens Goddard, A., Carrapa, B., & Aciar, R. H. (2020). Recognizing drainage reorganization in the stratigraphic record of the Neogene foreland basin of the Central Andes. Sedimentary Geology, 405, 105704. https://doi.org/10.1016/j.sedgeo.2020.105704

Sukhishvili, L., Forte, A. M., Merebashvili, G., Leonard, J., Whipple, K. X., Javakhishvili, Z., Heimsath, A., & Godoladze, T. (2021). Active deformation and Plio-Pleistocene fluvial reorganization of the western Kura fold–thrust belt, Georgia: Implications for the evolution of the Greater Caucasus Mountains. Geological Magazine, 158(4), 583–597. https://doi.org/10.1017/S0016756820000709

Tari, G., Blackbourn, G., Boote, D. r. d., Sachsenhofer, R. f., & Yukler, A. (2021). Exploration Plays in the Caucasus Region. Journal of Petroleum Geology, 44(3), 213–236. https://doi.org/10.1111/jpg.12791

Tofelde, S., Bernhardt, A., Guerit, L., & Romans, B. W. (2021). Times Associated With Source-to-Sink Propagation of Environmental Signals During Landscape Transience. Frontiers in Earth Science, 9. https://www.frontiersin.org/article/10.3389/feart.2021.628315

Trexler, C., Cowgill, E., Niemi, N. A., Vasey, D. A., & Godoladze, T. (2022). Tectonostratigraphy and major structures of the Georgian Greater Caucasus: Implications for structural architecture, along-strike continuity, and orogen evolution. Geosphere, 18(1), 211–240. https://doi.org/10.1130/GES02385.1

Trexler, C., Cowgill, E., Vasey, D., & Niemi, N. (2023). Total Shortening Estimates Across the Western Greater Caucasus Mountains from Balanced Cross Sections and Area Balancing. Tektonika, 1(2). https://doi.org/10.55575/tektonika2023.1.2.50

Tye, A. R., Niemi, N. A., Cowgill, E., Kadirov, F. A., & Babayev, G. R. (2022). Diverse Deformation Mechanisms and Lithologic Controls in an Active Orogenic Wedge: Structural Geology and Thermochronometry of the Eastern Greater Caucasus. Tectonics, 41(12). https://doi.org/10.1029/2022TC007349

Tye, A. R., Niemi, N. A., Safarov, R. T., Kadirov, F. A., & Babayev, G. R. (2020). Sedimentary response to a collision orogeny recorded in detrital zircon provenance of Greater Caucasus foreland basin sediments. Basin Research, bre.12499. https://doi.org/10.1111/bre.12499

Van Baak, C. G. C., Grothe, A., Richards, K., Stoica, M., Aliyeva, E., Davies, G. R., Kuiper, K. F., & Krijgsman, W. (2019). Flooding of the Caspian Sea at the intensification of Northern Hemisphere Glaciations. Global and Planetary Change, 174, 153–163. https://doi.org/10.1016/j.gloplacha.2019.01.007

Van Baak, C. G. C., Krijgsman, W., Magyar, I., Sztanó, O., Golovina, L. A., Grothe, A., Hoyle, T. M., Mandic, O., Patina, I. S., Popov, S. V., Radionova, E. P., Stoica, M., & Vasiliev, I. (2017). Paratethys response to the Messinian salinity crisis. Earth-Science Reviews, 172, 193–223. https://doi.org/10.1016/j.earscirev.2017.07.015

Van Baak, C. G. C., Radionova, E. P., Golovina, L. A., Raffi, I., Kuiper, K. F., Vasiliev, I., & Krijgsman, W. (2015). Messinian events in the Black Sea. Terra Nova, 27(6), 433–441. https://doi.org/10.1111/ter.12177

Van Baak, C. G. C., Vasiliev, I., Stoica, M., Kuiper, K. F., Forte, A. M., Aliyeva, E., & Krijgsman, W. (2013). A magnetostratigraphic time frame for Plio-Pleistocene transgressions in the South Caspian Basin, Azerbaijan. Global and Planetary Change, 103, 119–134. https://doi.org/10.1016/j.gloplacha.2012.05.004

van der Boon, A., van Hinsbergen, D. J. J., Rezaeian, M., Gürer, D., Honarmand, M., Pastor-Galán, D., Krijgsman, W., & Langereis, C. G. (2018). Quantifying Arabia–Eurasia convergence accommodated in the Greater Caucasus by paleomagnetic reconstruction. Earth and Planetary Science Letters, 482, 454–469. https://doi.org/10.1016/j.epsl.2017.11.025

van Hinsbergen, D. J. J., Trond, T. H., Schmid, S. M., Mat¸enco, L. C., Maffione, M., Vissers, R. L. M., Gürer, D., & Spakman, W. (2020). Orogenic architecture of the Mediterranean region and kinematic reconstruction of its tectonic evolution since the Triassic. Gondwana Research, 81, 79–229. https://doi.org/10.1016/j.gr.2019.07.009

Vasiliev, I., van der Meer, M. T. J., Stoica, M., Krijgsman, W., Reichart, G.-J., Lazarev, S., Butiseacă, G. A., Niedermeyer, E. M., Aliyeva, E., van Baak, C. G. C., & Mulch, A. (2022). Biomarkers reveal two paramount Pliocene-Pleistocene connectivity events in the Caspian Sea Basin. Palaeogeography, Palaeoclimatology, Palaeoecology, 587, 110802. https://doi.org/10.1016/j.palaeo.2021.110802

Vezzoli, G., Garzanti, E., Limonta, M., & Radeff, G. (2020). Focused erosion at the core of the Greater Caucasus: Sediment generation and dispersal from Mt. Elbrus to the Caspian Sea. Earth-Science Reviews, 200, 102987. https://doi.org/10.1016/j.earscirev.2019.102987

Vincent, S. J., Davies, C. E., Richards, K., & Aliyeva, E. (2010). Contrasting Pliocene fluvial depositional systems within the rapidly subsiding South Caspian Basin; a case study of the palaeo-Volga and palaeo-Kura river systems in the Surakhany Suite, Upper Productive Series, onshore Azerbaijan. Marine and Petroleum Geology, 27(10), 2079–2106. https://doi.org/10.1016/j.marpetgeo.2010.09.007

Vincent, S. J., Somin, M. L., Carter, A., Vezzoli, G., Fox, M., & Vautravers, B. (2020). Testing Models of Cenozoic Exhumation in the Western Greater Caucasus. Tectonics, 39(2), e2018TC005451. https://doi.org/10.1029/2018TC005451

Zonenshain, L. P., & Pichon, X. (1986). Deep basins of the Black Sea and Caspian Sea as remnants of Mesozoic back-arc basins. Tectonophysics, 123(1), 181–211. https://doi.org/10.1016/0040-1951(86)90197-6

How to cite: Fowler, K., & Forte, A. M. (2024). Distinguishing climate and tectonic signals in the stratigraphy of the Kura Basin, the southeastern foreland of the Greater Caucasus. Sedimentologika, 2(1), 1-29. https://doi.org/10.57035/journals/sdk.2024.e21.1272

CC BY